
Conformal Prediction for Class-wise Coverage via Augmented Label Rank Calibration

Yuanjie Shi

Washington State University

Subhankar Ghosh

Washington State University

Taha Belkhouja

Washington State University

Janardhan Rao Doppa

Washington State University

Yan Yan

Washington State University

Abstract

Conformal prediction (CP) is an emerging uncertainty quantification framework that allows us to construct a prediction set to cover the true label with a pre-specified marginal or conditional probability. Although the valid coverage guarantee has been extensively studied for classification problems, CP often produces large prediction sets which may not be practically useful. This issue is exacerbated for the setting of class-conditional coverage on classification tasks with many and/or imbalanced classes. This paper proposes the Rank Calibrated Class-conditional CP (RC3P) algorithm to reduce the prediction set sizes to achieve class-conditional coverage, where the valid coverage holds for each class. In contrast to the standard class-conditional CP (CCP) method that uniformly thresholds the class-wise conformity score for each class, the augmented label rank calibration step allows RC3P to selectively iterate this class-wise thresholding subroutine only for a subset of classes whose class-wise top- k error is small. We prove that agnostic to the classifier and data distribution, RC3P achieves class-wise coverage. We also show that RC3P reduces the size of prediction sets compared to the CCP method. Comprehensive experiments on multiple real-world datasets demonstrate that RC3P achieves class-wise coverage and 26.25% ↓ reduction in prediction set sizes on average.

1 Introduction

Safe deployment of machine learning (ML) models in high stakes applications such as medical diagnosis requires theoretically-sound uncertainty estimates. Conformal prediction (CP) [11] is an emerging uncertainty quantification framework that constructs a prediction set of candidate output values such that the true output is present with a pre-specified level (e.g., $\geq 90\%$) of the marginal or conditional probability [39, 40]. A promising property of CP is the model-agnostic and distribution-free *coverage validity* under certain notions [42]. For example, marginal coverage is the commonly studied validity notion [9, 20, 39], while conditional coverage is a stronger notion. There is a general taxonomy to group data (i.e., input-output pairs) into categories and to study the valid coverage for each group (i.e., the group-wise validity) [44, 11]. This paper focuses on the specific notion of class-conditional coverage that guarantees coverage for each class individually, which is important for imbalanced classification tasks with many and/or imbalanced classes (e.g., medical applications) [41, 47, 48].

In addition to the coverage validity, *predictive efficiency* is another important criterion for CP [42, 46], which refers to the size of the prediction sets. Both coverage validity and predictive efficiency are used together to measure the performance of CP methods [20, 38, 9, 33, 1, 43]. Since the two measures are competing [20], our goal is to guarantee the coverage validity with high predictive efficiency, i.e.,

small prediction sets [42, 9, 43]. Some studies improved the predictive efficiency under the marginal coverage setting using new conformity score function [20, 35] and new calibration procedures [40, 43, 19, 36]. However, it is not known if these methods will benefit the predictive efficiency for the class-conditional coverage setting. A very recent work [33] proposed the cluster CP method to achieve *approximate* class-conditional coverage. It empirically improves predictive efficiency over the baseline class-wise CP method (i.e., each class is one cluster) [30], but the approximation guarantee for class-wise coverage is *model-dependent* (i.e., requires certain assumptions on the model). The main question of this paper is: *how can we develop a model-agnostic CP algorithm that guarantees the class-wise coverage with improved predictive efficiency (i.e., small prediction sets)?*

To answer this question, we propose a novel approach referred to as *Rank Calibrated Class-conditional CP (RC3P)* that guarantees the class-wise coverage with small expected prediction sets. The class-conditional coverage validity of RC3P is agnostic to the data distribution and the underlying ML model, while the improved predictive efficiency depends on very mild conditions of the given trained classifier. The main ingredient behind the RC3P method is the label rank calibration strategy augmented with the standard conformal score calibration from the class-wise CP (CCP) [30, 21].

The CCP method finds the class-wise quantiles of non-conformity scores on calibration data. To produce the prediction set for a new test input X_{test} , it pairs X_{test} with each candidate class label y and includes the label y if the non-conformity score of the pair (X_{test}, y) is less than or equal to the corresponding class-wise quantile associated with y . Thus, CCP constructs the prediction set by uniformly iterating over *all* candidate labels. In contrast, the label rank calibration allows RC3P to selectively iterate this class-wise thresholding subroutine only if the label y is ranked by the classifier $f(X_{\text{test}})$ (e.g., $f(\cdot)$ denotes the softmax prediction) in the top k_y candidates, where the value of k_y is calibrated for each label y individually according to the class-wise top- k_y error. In other words, given X_{test} , RC3P enables standard class-wise conformal thresholding for the sufficiently certain class labels only (as opposed to all labels). Our theory shows that the class-wise coverage provided by RC3P is agnostic to the data distribution and the underlying ML model. Moreover, under a very mild condition, RC3P guarantees improved predictive efficiency over the baseline CCP method.

Contributions. The main contributions of this paper are:

- We design a novel algorithm RC3P that augments the label rank calibration strategy to the standard conformal score calibration step. To produce prediction sets for new inputs, it selectively performs class-wise conformal thresholding only on a subset of classes based on their corresponding calibrated label ranks.
- We develop theoretical analysis to show that RC3P guarantees class-wise coverage, which is agnostic to the data distribution and trained classifier. Moreover, it provably produces smaller average prediction sets over the baseline CCP method [30].
- We perform extensive experiments on multiple imbalanced classification datasets and show that RC3P achieves the class-wise coverage with significantly improved predictive efficiency over the existing class-conditional CP baselines (26.25% reduction in the prediction size on average on all four datasets or 35% reduction excluding CIFAR-10). The code is available at <https://github.com/YuanjieSh/RC3P>.

2 Related Work

Precise uncertainty quantification of machine learning based predictions is necessary in high-stakes decision-making applications. It is especially challenging for imbalanced classification tasks. Although many imbalanced classification learning algorithms [5, 29] are proposed, e.g., re-sampling [22, 24, 25, 23, 26] and re-weighting [27, 28], they do not provide uncertainty quantification with rigorous guarantees over predictions for each class.

Conformal prediction [14, 11] is a model-agnostic and distribution-free framework for uncertainty quantification by producing prediction sets that cover the true output with a pre-specified probability, which means CP could provide valid coverage guarantee with any underlying model and data distribution [61, 62, 63]. Many CP algorithms are proposed for regression [58, 34, 16, 60], classification [38, 20, 52, 53], structured prediction [49, 50, 51, ?], online learning [?, 59], and covariate shift

Table 1: Key notations used in this paper.

Notation	Meaning
$X \in \mathcal{X}$	Input example
$Y \in \mathcal{Y}$	The ground-truth label
f	The soft classifier
Δ_+^K	The K -dimensional probability simplex
$f(X)_y$	The predicted confidence on class y
ϵ_y^k	The class-wise top- k error for class y from f
$r_f(X, Y)$	The rank of Y predicted by $f(X)$
\mathcal{D}_{tr}	Training data
\mathcal{D}_{cal}	Calibration data
$\mathcal{D}_{\text{test}}$	Test data
n_y	The number of calibration examples for class y
$V(X, Y)$	Non-conformity scoring function
$\mathcal{C}_{1-\alpha}(X_{\text{test}})$	Prediction set for input X_{test}
α	Target mis-coverage rate
$\widehat{\alpha}_y$	Nominal mis-coverage rate for class y

[?, 17, 54] settings. *Coverage validity* and *predictive efficiency* are two common and competing desiderata for CP methods [20]. Thus, small prediction sets are favorable whenever the coverage validity is guaranteed [42, 9, 43], e.g., human and machine learning collaborative systems [41, 47, 48]. Recent work¹ improved the predictive efficiency for marginal coverage by designing new conformity score [20, 35] and calibration procedures [40, 43, 19, 36]. These methods can be combined with class-conditional CP methods including RC3P as we demonstrate in our experiments, but the effect on predictive efficiency is not clear.

In general, the methods designed for a specific coverage validity notion are not necessarily compatible with another notion of coverage, such as object-conditional coverage [30], class-conditional coverage [30], local coverage [45] which are introduced and studied in the prior CP literature [44, 11, 42, 33, 37]. The standard class-conditional CP method in [30, 18] guarantees the class-wise coverage, but does not particularly aim to reduce the size of prediction sets. The cluster CP method [33] which performs CP over clusters of labels achieves a cluster-conditional coverage that approximates the class-conditional guarantee, but requires some assumptions on the underlying clustering model.

Our goal is to develop a provable class-conditional CP algorithm with small prediction sets to guarantee the class-wise coverage that is agnostic to the underlying model.

3 Notations, Background, and Problem Setup

Notations. Suppose (X, Y) is a data sample where $X \in \mathcal{X}$ is an input from the input space \mathcal{X} , and $Y \in \mathcal{Y} = \{1, 2, \dots, K\}$ is the ground-truth label with K candidate classes. Assume (X, Y) is randomly drawn from an underlying distribution \mathcal{P} defined on $\mathcal{X} \times \mathcal{Y}$, where we denote $p_y = \mathbb{P}_{XY}[Y = y]$. Let $f : \mathcal{X} \rightarrow \Delta_+^K$ denote a soft classifier (e.g., a soft-max classifier) that produces prediction scores for all candidate classes on any given input X , where Δ_+^K denote the K -dimensional probability simplex and $f(X)_y$ denotes the predicted confidence for class y . We define the class-wise top- k error for class y from the trained classifier f as $\epsilon_y^k = \mathbb{P}\{r_f(X, Y) > k | Y = y\}$, where $r_f(X, Y) = \sum_{l=1}^K \mathbb{1}[f(X)_l \geq f(X)_Y]$ returns the rank of Y predicted by $f(X)$ in a descending order, and $\mathbb{1}[\cdot]$ is an indicator function. We are provided with a training set \mathcal{D}_{tr} for training the classifier f , and a calibration set $\mathcal{D}_{\text{cal}} = \{(X_i, Y_i)\}_{i=1}^n$ for CP. Let $\mathcal{I}_y = \{i : Y_i = y, \text{ for all } (X_i, Y_i) \in \mathcal{D}_{\text{cal}}\}$ and $n_y = |\mathcal{I}_y|$ denote the number of calibration examples for class y .

Problem Setup of CP. Let $V : \mathcal{X} \times \mathcal{Y} \rightarrow \mathbb{R}$ denote a *non-conformity* scoring function to measure how different a new example is from old ones [11]. It is employed to compare a given testing sample

¹A concurrent work by Huang and colleagues [64] studied a method named sorted adaptive prediction sets which uses label ranking information to improve the predictive efficiency in the marginal coverage setting.

$(X_{\text{test}}, Y_{\text{test}})$ with a set of calibration data \mathcal{D}_{cal} : if the non-conformity score is large, then $(X_{\text{test}}, Y_{\text{test}})$ conforms less to calibration samples. Prior work has considered the design of good non-conformity scoring functions, e.g., [21, 15, 9]. In this paper, we focus on the scoring functions of *Adaptive Prediction Sets* (APS) proposed in [9] and *Regularized APS* (RAPS) proposed in [20] for classification based on the ordered probabilities of f and true label rank $r_f(X, Y)$. For the simplicity of notation, we denote the non-conformity score of the i -th calibration example as $V_i = V(X_i, Y_i)$.

Given a input X , we sort the predicted probability for all classes $\{1, \dots, K\}$ of the classifier f such that $1 \geq f(X)_{(1)} \geq \dots \geq f(X)_{(K)} \geq 0$ are ordered statistics, where $f(X)_{(k)}$ denotes the k -th largest prediction. The APS [9] score for a sample (X, Y) is computed as follows:

$$V(X, Y) = \sum_{l=1}^{r_f(X, Y)-1} f(X)_{(l)} + U \cdot f(X)_{(r_f(X, Y))},$$

where $U \in [0, 1]$ is a uniform random variable to break ties. We also consider its regularized variant RAPS [20], which additionally includes a rank-based regularization $\lambda(r_f(X, Y) - k_{\text{reg}})^+$ to the above equation, where $(\cdot)^+ = \max\{0, \cdot\}$ denotes the hinge loss, λ and k_{reg} are two hyper-parameters.

For a target coverage $1 - \alpha$, we find the corresponding empirical quantile on calibration data \mathcal{D}_{cal} defined as

$$\hat{Q}_{1-\alpha} = \min \left\{ t : \sum_{i=1}^n \frac{1}{n} \cdot \mathbb{1}[V_i \leq t] \geq 1 - \alpha \right\},$$

which can be determined by finding the $\lceil (1 - \alpha)(1 + n) \rceil$ -th smallest value of $\{V_i\}_{i=1}^n$. The prediction set of a testing input X_{test} can be constructed by thresholding with $\hat{Q}_{1-\alpha}$:

$$\hat{\mathcal{C}}_{1-\alpha}(X_{\text{test}}) = \{y \in \mathcal{Y} : V(X_{\text{test}}, y) \leq \hat{Q}_{1-\alpha}\}.$$

Therefore, $\hat{\mathcal{C}}_{1-\alpha}$ gives a *marginal coverage* guarantee [9, 20]: $\mathbb{P}_{(X, Y) \sim \mathcal{P}}\{Y \in \hat{\mathcal{C}}_{1-\alpha}(X)\} \geq 1 - \alpha$. To achieve the *class-conditional coverage*, standard CCP [30] uniformly iterates the class-wise thresholding subroutine with the class-wise quantiles $\{\hat{Q}_{1-\alpha}^{\text{class}}(y)\}_{y \in \mathcal{Y}}$:

$$\begin{aligned} \hat{\mathcal{C}}_{1-\alpha}^{\text{CCP}}(X_{\text{test}}) &= \{y \in \mathcal{Y} : V(X_{\text{test}}, y) \leq \hat{Q}_{1-\alpha}^{\text{class}}(y)\}, \\ \text{where } \hat{Q}_{1-\alpha}^{\text{class}}(y) &= \min \left\{ t : \sum_{i \in \mathcal{I}_y} \frac{1}{n_y} \cdot \mathbb{1}[V_i \leq t] \geq 1 - \alpha \right\}. \end{aligned} \quad (1)$$

Specifically, CCP pairs X_{test} with each candidate class label y , and includes y in the prediction set $\hat{\mathcal{C}}_{1-\alpha}^{\text{CCP}}(X_{\text{test}})$ if $V(X_{\text{test}}, y) \leq \hat{Q}_{1-\alpha}^{\text{class}}(y)$ holds. After going through all candidate class labels $y \in \mathcal{Y}$, it achieves the class-wise coverage for any $y \in \mathcal{Y}$ [30, 21]:

$$\mathbb{P}_{(X, Y) \sim \mathcal{P}}\{Y \in \hat{\mathcal{C}}_{1-\alpha}^{\text{CCP}}(X) | Y = y\} \geq 1 - \alpha. \quad (2)$$

CCP produces large prediction sets which are not useful in practice. Therefore, our goal is to develop a provable CP method that provides class-conditional coverage and constructs smaller prediction sets than those from CCP. We summarize all the notations in Table 1.

4 Rank Calibrated Class-Conditional CP

We first explain the proposed *Rank Calibrated Class-conditional Conformal Prediction (RC3P)* algorithm and present its model-agnostic coverage guarantee. Next, we provide the theoretical analysis for the provable improvement of predictive efficiency of RC3P over the CCP method.

4.1 Algorithm and Model-Agnostic Coverage Analysis

We start with the motivating discussion about the potential drawback of the standard CCP method in terms of *predictive efficiency*. Equation (1) shows that, for a given test input X_{test} , CCP likely contains some uncertain labels due to the uniform iteration over each class label $y \in \mathcal{Y}$ to check if y should be included into the prediction set or not. For example, given a class label y and two

Algorithm 1 RC3P Method for Class-Conditional CP

- 1: **Input:** Mis-coverage rate $\alpha \in (0, 1)$, top- k errors ϵ_y^k for all classes and ranks $y, k \in \{1, \dots, K\}$
- 2: Randomly split data into train \mathcal{D}_{tr} and calibration \mathcal{D}_{cal} and train the classifier f on \mathcal{D}_{tr}
- 3: **for** $y \in \{1, \dots, K\}$ **do**
- 4: Compute $\{V_i\}_{i=1}^{n_y}$ for all $(X_i, Y_i) \in \mathcal{D}_{\text{cal}}$ such that $Y_i = y$
- 5: Configure calibrated label rank $\hat{k}(y)$ and nominal error $\hat{\alpha}_y$:
- 6: Option I (model-agnostic coverage):

$$\hat{k}(y) \in \{k : \epsilon_y^k < \alpha\}, 0 \leq \hat{\alpha}_y \leq \alpha - \epsilon_y^{\hat{k}(y)}, \text{ as per Eq (4)}$$
- 7: Option II (model-agnostic coverage + improved predictive efficiency):

$$\hat{k}(y) = \min\{k : \epsilon_y^k < \alpha\}, \hat{\alpha}_y = \alpha - \epsilon_y^{\hat{k}(y)}, \text{ as per Eq (7)}$$
- 8: $\hat{Q}_{1-\hat{\alpha}_y}^{\text{class}}(y) \leftarrow \lceil (1 - \hat{\alpha}_y)(1 + n_y) \rceil$ -th smallest value in $\{V_i\}_{i=1}^{n_y}$ according to Eq (1)
- 9: **end for**
- 10: Construct $\hat{\mathcal{C}}_{1-\alpha}^{\text{RC3P}}(X_{\text{test}})$ with $\hat{Q}_{1-\hat{\alpha}_y}^{\text{class}}(y)$ and $\hat{k}(y)$ for a test input X_{test} using Eq (3)

test samples X_1, X_2 , suppose their APS scores are $V(X_1, y) = 0.9, V(X_2, y) = 0.8$, with ranks $r_f(X_1, y) = 1, r_f(X_2, y) = 5$. Furthermore, if $\hat{Q}_{1-\alpha}^{\text{class}}(y) = 0.85$, then by (1) for CCP, we know that $y \notin \hat{\mathcal{C}}_{1-\alpha}^{\text{CCP}}(X_1)$ and $y \in \hat{\mathcal{C}}_{1-\alpha}^{\text{CCP}}(X_2)$, even though $f(X_1)$ ranks y at the #1 class label for X_1 with a very high confidence $f(X_1)_y = 0.9$ and CCP can still achieve the valid class-conditional coverage. We argue that, the principle of CCP to scans all $y \in \mathcal{Y}$ uniformly can easily result in large prediction sets, which is detrimental to the effectiveness of human-ML collaborative systems [3, 2].

Consequently, to improve the predictive efficiency of CCP (i.e., reduce prediction set sizes), it is reasonable to include label rank information in the calibration procedure to adjust the distribution of non-conformity scores for predictive efficiency. As mentioned in the previous sections, better scoring functions have been proposed to improve the predictive efficiency for marginal coverage, e.g., RAPS. However, directly applying RAPS for class-wise coverage presents challenges: 1) tuning its hyper-parameters for each class requires extra computational overhead, and 2) fixing its hyper-parameters for all classes overlooks the difference between distributions of different classes. Moreover, for the approximate class-conditional coverage achieved by cluster CP [33], it still requires some assumptions on the underlying model (i.e., it is not fully model-agnostic).

Therefore, the key idea of our proposed RC3P algorithm (outlined in Algorithm 1) is to refine the class-wise calibration procedure using a label rank calibration strategy augmented to the standard conformal score calibration, to enable adaptivity to various classes. Specifically, in contrast to CCP, RC3P selectively activates the class-wise thresholding subroutine in (1) according to their class-wise top- k error ϵ_y^k for class y . RC3P produces the prediction set for a given test input X_{test} with two calibration schemes (one for conformal score and another for label rank) as shown below:

$$\hat{\mathcal{C}}_{1-\alpha}^{\text{RC3P}}(X_{\text{test}}) = \{y \in \mathcal{Y} : \underbrace{V(X_{\text{test}}, y) \leq \hat{Q}_{1-\hat{\alpha}_y}^{\text{class}}(y)}_{\text{conformal score calibration}}, \underbrace{r_f(X_{\text{test}}, y) \leq \hat{k}(y)}_{\text{label rank calibration}}\}, \quad (3)$$

where $\hat{Q}_{1-\hat{\alpha}_y}^{\text{class}}(y)$ and $\hat{k}(y)$ are score and label rank threshold for class y , respectively. In particular, $\hat{k}(y)$ controls the class-wise uncertainty adaptive to each class y based on the top- k error $\epsilon_y^{\hat{k}(y)}$ of the classifier. By determining $\hat{k}(y)$, the top k predicted class labels of $f(X_{\text{test}})$ will more likely cover the true label Y_{test} , making the augmented label rank calibration filter out the class labels y that have a high rank (larger $r_f(X, y)$). As a result, given all test input and label pairs $\{(X_{\text{test}}, y)\}_{y \in \mathcal{Y}}$, RC3P performs score thresholding using class-wise quantiles only on a subset of reliable test pairs.

Determining $\hat{k}(y)$ and $\hat{\alpha}_y$ for model-agnostic valid coverage. For class y , intuitively, we would like a value for $\hat{k}(y)$ such that the corresponding top- $\hat{k}(y)$ error is smaller than α , so that it is possible to guarantee valid coverage (recall $\mathbb{P}\{A, B\} = \mathbb{P}\{A\} \cdot \mathbb{P}\{B|A\}$). Since a larger $\hat{k}(y)$ gives a smaller $\epsilon_y^{\hat{k}(y)}$ until $\epsilon_y^{\hat{k}(y)} = 0$, it is guaranteed to find a value for $\hat{k}(y)$, in which the corresponding $\epsilon_y^{\hat{k}(y)} < \alpha$. As a result, given all test input and label pairs $\{(X_{\text{test}}, y)\}_{y \in \mathcal{Y}}$, RC3P performs score thresholding using class-wise quantiles only on a subset of reliable test pairs and filters out the class labels y that

have a high rank (larger $r_f(X, y)$). The following result formally shows the principle to configure $\hat{k}(y)$ and $\hat{\alpha}_y$ to guarantee the class-wise coverage that is agnostic to the underlying model.

Theorem 4.1. (*Class-conditional coverage of RC3P*) Suppose that selecting $\hat{k}(y)$ values result in the class-wise top- k error $\epsilon_y^{\hat{k}(y)}$ for each class $y \in \mathcal{Y}$. For a target class-conditional coverage $1 - \alpha$, if we set $\hat{\alpha}_y$ and $\hat{k}(y)$ in RC3P (3) in the following ranges:

$$\hat{k}(y) \in \{k : \epsilon_y^k < \alpha\}, \quad 0 \leq \hat{\alpha}_y \leq \alpha - \epsilon_y^{\hat{k}(y)}, \quad (4)$$

then RC3P can achieve the class-conditional coverage for every $y \in \mathcal{Y}$:

$$\mathbb{P}_{(X,Y) \sim \mathcal{P}}\{Y \in \hat{\mathcal{C}}_{1-\alpha}^{RC3P}(X) | Y = y\} \geq 1 - \alpha.$$

4.2 Analysis of Predictive Efficiency for RC3P

We further analyze the predictive efficiency of RC3P: under what conditions RC3P can produce a smaller expected prediction set size compared to CCP, when both achieve the same $(1 - \alpha)$ -class-conditional coverage. We investigate how to choose the value of $\hat{\alpha}_y$ and $\hat{k}(y)$ from the feasible ranges in (4) to achieve the best predictive efficiency using RC3P.

Lemma 4.2. (*Trade-off condition for improved predictive efficiency of RC3P*) Suppose $\hat{\alpha}_y$ and $\hat{k}(y)$ satisfy (4) in Theorem 4.1. If the following inequality holds for any $y \in \mathcal{Y}$:

$$\mathbb{P}_{X_{\text{test}}}\left[V(X_{\text{test}}, y) \leq \hat{Q}_{1-\hat{\alpha}}^{\text{class}}(y), r_f(X_{\text{test}}, y) \leq \hat{k}(y)\right] \leq \mathbb{P}_{X_{\text{test}}}\left[V(X_{\text{test}}, y) \leq \hat{Q}_{1-\alpha}^{\text{class}}(y)\right], \quad (5)$$

then RC3P produces smaller expected prediction sets than CCP, i.e.,

$$\mathbb{E}_{X_{\text{test}}}\left[\left|\hat{\mathcal{C}}_{1-\hat{\alpha}}^{RC3P}(X_{\text{test}})\right|\right] \leq \mathbb{E}_{X_{\text{test}}}\left[\left|\hat{\mathcal{C}}_{1-\alpha}^{CCP}(X_{\text{test}})\right|\right].$$

Remark. The above result demonstrates that when both RC3P and CCP achieve the target $1 - \alpha$ class-conditional coverage, under the condition of (5), RC3P produces smaller prediction sets than CCP. In fact, this condition implies that the combined (conformity score and label rank) calibration of RC3P tends to include less labels with high rank or low confidence from the classifier. In contrast, the CCP method tends to include relatively more uncertain labels into the prediction set, where their ranks are high and the confidence of the classifier is low. Now we can interpret the condition (5) by defining a condition number, termed as σ_y :

$$\sigma_y = \frac{\mathbb{P}_{X_{\text{test}}}\left[V(X_{\text{test}}, y) \leq \hat{Q}_{1-\hat{\alpha}}^{\text{class}}(y), r_f(X_{\text{test}}, y) \leq \hat{k}(y)\right]}{\mathbb{P}_{X_{\text{test}}}\left[V(X_{\text{test}}, y) \leq \hat{Q}_{1-\alpha}^{\text{class}}(y)\right]}. \quad (6)$$

In other words, if we can verify that $\sigma_y \leq 1$ for all y , then RC3P can improve the predictive efficiency over CCP. Furthermore, if σ_y is fairly small, then the efficiency improvement can be even more significant. To verify this condition, our comprehensive experiments (Section 5.2, Figure 3) show that σ_y values are much smaller than 1 on real-world data. These results demonstrate the practical utility of our theoretical analysis to produce small prediction sets using RC3P. Note that the reduction in prediction set size of RC3P over CCP is proportional to how small the σ_y values are.

Theorem 4.3. (*Conditions of improved predictive efficiency for RC3P*) Define $D = \mathbb{P}[r_f(X, y) \leq \hat{k}(y) | Y \neq y]$, and $\bar{r}_f(X, y) = \lfloor \frac{r_f(X, y) + 1}{2} \rfloor$. Denote $B = \mathbb{P}[f(X)_{(\bar{r}_f(X, y))} \leq \hat{Q}_{1-\alpha}^{\text{class}}(y) | Y \neq y]$ if V is APS, or $B = \mathbb{P}[f(X)_{(\bar{r}_f(X, y))} + \lambda \leq \hat{Q}_{1-\alpha}^{\text{class}}(y) | Y \neq y]$ if V is RAPS. If $B - D \geq \frac{p_y}{1-p_y}(\alpha - \epsilon_y^{\hat{k}(y)})$, then $\sigma_y \leq 1$.

Remark. The above result further analyzes when the condition in Eq (5) of Lemma 4.2 (or equivalently, $\sigma_y \leq 1$) holds to guarantee the improved predictive efficiency. Specifically, the condition $B - D \geq \frac{p_y}{1-p_y}(\alpha - \epsilon_y^{\hat{k}(y)})$ of Theorem 4.3 can be realized by two ways: (i) making LHS $B - D$ as large as possible; (ii) making the RHS $\frac{p_y}{1-p_y}(\alpha - \epsilon_y^{\hat{k}(y)})$ as small as possible. To this end, we can set Line 7 in Algorithm 1 in the following way:

$$\hat{k}(y) = \min\{k : \epsilon_y^k < \alpha\}, \quad \hat{\alpha}_y = \alpha - \epsilon_y^{\hat{k}(y)}. \quad (7)$$

Therefore, this setting ensures $\sigma_y \leq 1$ and as a result improved predictive efficiency.

5 Experiments and Results

We present the empirical evaluation of the RC3P algorithm and demonstrate its effectiveness in achieving class-conditional coverage to produce small prediction sets. We conduct experiments using two baselines (CCP and Cluster-CP), four datasets (each with three imbalance types and five imbalance ratios), and two machine learning models (trained for 50 epochs and 200 epochs, with 200 epochs being our main experimental setting). Additionally, we use two scoring functions (APS and RAPS) and set three different α values ($\alpha \in 0.1, 0.05, 0.01$, with $\alpha = 0.1$ as our main setting).

5.1 Experimental Setup

Classification datasets. We consider four datasets: CIFAR-10, CIFAR-100 [6], mini-ImageNet [31], and Food-101 [32] by using the standard training and validation split. We employ the same methodology as [10, 5, 4] to create an imbalanced long-tail setting for each dataset as a harder challenge: 1) We use the original training split as a training set for training f with training samples (n_{tr} is defined as the number of training samples), and randomly split the original (balanced) validation set into calibration samples and testing samples. 2) We define an imbalance ratio ρ , the ratio between the sample size of the smallest and largest class: $\rho = \frac{\min_i \{\# \text{samples in class } i\}}{\max_i \{\# \text{samples in class } i\}}$. 3) For each training set, we create three different imbalanced distributions using three decay types over the class indices $c \in \{1, \dots, K\}$: (a) An exponential-based decay (EXP) with $\frac{n_{tr}}{K} \times \rho^{\frac{c}{K}}$ examples in class c , (b) A polynomial-based decay (POLY) with $\frac{n_{tr}}{K} \times \frac{1}{\sqrt{\frac{c}{10\rho} + 1}}$ examples in class c , and (c) A majority-based decay (MAJ) with $\frac{n_{tr}}{K} \times \rho$ examples in classes $c > 1$. We keep the calibration and test set balanced and unchanged. We provide an illustrative example of the three decay types in Appendix (Section B.3, Figure 4). Towards a more complete comparison, we also employ balanced datasets. Following Cluster-CP², we employ CIFAR-100, Places365 [65], iNaturalist[66], and ImageNet[67].

Deep neural network models. We consider ResNet-20 [8] as the main architecture to train classifiers for imbalanced classification datasets. To handle imbalanced data, we employ the training algorithm “LDAM” proposed by [5] that assigns different margins to classes, where larger margins are assigned to minority classes in the loss function. We follow the training strategy in [5] where all models are trained with 200 epochs. The class-wise performance with three imbalance types and imbalance ratios $\rho = 0.5$ and $\rho = 0.1$ on four datasets are evaluated (see Appendix B.1). We also train models with 50 epochs and the corresponding APSS results are reported in Appendix B.8.

For balanced datasets, we follow the same settings from Cluster-CP, which uses IMAGENET1K_V2 as pre-trained weights from PyTorch [68] and then fine-tune models with ResNet-50 for all datasets except ImageNet. For ImageNet, we use SimCLR-v2 [69] as training models.

CP baselines. We consider three CP methods: **1)** CCP which estimates class-wise score thresholds and produces prediction set using Equation (1); **2)** Cluster-CP [33] that performs calibration over clusters to reduce prediction set sizes; and **3)** RC3P that produces prediction set using Equation (3). All CP methods are built on the same classifier and non-conformity scoring function for a fair comparison. We employ the three common scoring functions: APS [9], RAPS [20], and HPS [18]. We set $\alpha = 0.1$ as our main experiment setting and also report other experiment results of different α values (See Appendix B.7). Meanwhile, the hyper-parameters for each baseline are tuned according to their recommended ranges based on the same criterion (see Appendix B.2). We repeat experiments over 10 different random calibration-testing splits and report the mean and standard deviation.

Evaluation methodology. We use the target coverage $1 - \alpha = 90\%$ class-conditional coverage for CCP, Cluster-CP, and RC3P. We compute three evaluation metrics on the testing set:

- *Under Coverage Ratio (UCR).*

$$\text{UCR} := \sum_{c \in [K]} \mathbb{1} \left[\frac{\mathbb{E}_{X_{\text{test}}} \mathbb{1}[y \in \hat{\mathcal{C}}_{1-\alpha}(x) \text{ s.t. } y = c]}{\mathbb{E}_{X_{\text{test}}} \mathbb{1}[y = c]} < 1 - \alpha \right] / K.$$

²<https://github.com/tiffanyding/class-conditional-conformal/tree/main>

Table 2: **Imbalanced classification data experiment on CIFAR-10, CIFAR-100, mini-ImageNet, Food-101.** APSS results comparing CCP, Cluster-CP, and RC3P with ResNet-20 model trained with 200 epochs under different imbalance types and ratios when $\alpha = 0.1$. For a fair comparison of APSS, we set UCR of RC3P the same as or smaller (more restrictive) than that of CCP and Cluster-CP under 0.16 on CIFAR-10 and 0.03 on other datasets. The specified UCR values are in Table 6 and 7 of Appendix B.4 and B.5. The APSS results show that RC3P significantly outperforms CCP and Cluster-CP in terms of average prediction set size with 24.47% (four datasets) or 32.63% (excluding CIFAR-10) reduction over $\min\{\text{CCP}, \text{cluster-CP}\}$.

Conformity Score	Methods	EXP		POLY		MAJ	
		$\rho = 0.5$	$\rho = 0.1$	$\rho = 0.5$	$\rho = 0.1$	$\rho = 0.5$	$\rho = 0.1$
CIFAR-10							
APS	CCP	1.555 \pm 0.010	1.855 \pm 0.014	1.538 \pm 0.010	1.776 \pm 0.012	1.840 \pm 0.020	2.629 \pm 0.013
	Cluster-CP	1.714 \pm 0.018	2.162 \pm 0.015	1.706 \pm 0.014	1.928 \pm 0.013	1.948 \pm 0.023	3.220 \pm 0.020
	RC3P	1.555 \pm 0.010	1.855 \pm 0.014	1.538 \pm 0.010	1.776 \pm 0.012	1.840 \pm 0.020	2.629 \pm 0.013
RAPS	CCP	1.555 \pm 0.010	1.855 \pm 0.014	1.538 \pm 0.010	1.776 \pm 0.012	1.840 \pm 0.020	2.632 \pm 0.012
	Cluster-CP	1.714 \pm 0.018	2.162 \pm 0.015	1.706 \pm 0.014	1.929 \pm 0.013	1.787 \pm 0.019	2.968 \pm 0.024
	RC3P	1.555 \pm 0.010	1.855 \pm 0.014	1.538 \pm 0.010	1.776 \pm 0.012	1.840 \pm 0.020	2.632 \pm 0.012
HPS	CCP	1.144 \pm 0.005	1.324 \pm 0.007	1.137 \pm 0.003	1.243 \pm 0.005	1.272 \pm 0.008	1.936 \pm 0.010
	Cluster-CP	1.214 \pm 0.008	1.508 \pm 0.010	1.211 \pm 0.004	1.354 \pm 0.005	1.336 \pm 0.009	2.312 \pm 0.025
	RC3P	1.144 \pm 0.005	1.324 \pm 0.007	1.137 \pm 0.003	1.243 \pm 0.005	1.272 \pm 0.008	1.936 \pm 0.010
CIFAR-100							
APS	CCP	44.224 \pm 0.341	50.969 \pm 0.345	49.889 \pm 0.353	64.343 \pm 0.237	44.194 \pm 0.514	64.642 \pm 0.535
	Cluster-CP	29.238 \pm 0.609	37.592 \pm 0.857	38.252 \pm 0.353	52.391 \pm 0.595	31.518 \pm 0.335	50.883 \pm 0.673
	RC3P	17.705 \pm 0.004	21.954 \pm 0.005	23.048 \pm 0.008	33.185 \pm 0.005	18.581 \pm 0.007	32.699 \pm 0.005
RAPS	CCP	44.250 \pm 0.342	50.970 \pm 0.345	49.886 \pm 0.353	64.332 \pm 0.236	48.343 \pm 0.353	64.663 \pm 0.535
	Cluster-CP	29.267 \pm 0.612	37.795 \pm 0.862	38.258 \pm 0.320	52.374 \pm 0.592	31.513 \pm 0.325	50.379 \pm 0.684
	RC3P	17.705 \pm 0.004	21.954 \pm 0.005	23.048 \pm 0.008	33.185 \pm 0.005	18.581 \pm 0.006	32.699 \pm 0.006
HPS	CCP	41.351 \pm 0.242	49.469 \pm 0.344	48.063 \pm 0.376	63.963 \pm 0.277	46.125 \pm 0.351	64.371 \pm 0.564
	Cluster-CP	27.566 \pm 0.555	35.528 \pm 0.979	36.101 \pm 0.565	51.333 \pm 0.776	29.323 \pm 0.363	50.519 \pm 0.679
	RC3P	20.363 \pm 0.006	25.212 \pm 0.010	25.908 \pm 0.007	36.951 \pm 0.018	21.149 \pm 0.006	35.606 \pm 0.005
mini-ImageNet							
APS	CCP	26.676 \pm 0.171	26.111 \pm 0.194	26.626 \pm 0.133	26.159 \pm 0.208	27.313 \pm 0.154	25.629 \pm 0.207
	Cluster-CP	25.889 \pm 0.301	25.253 \pm 0.346	26.150 \pm 0.393	25.633 \pm 0.268	26.918 \pm 0.241	25.348 \pm 0.334
	RC3P	18.129 \pm 0.003	17.082 \pm 0.002	17.784 \pm 0.003	17.465 \pm 0.003	18.111 \pm 0.002	17.167 \pm 0.004
RAPS	CCP	26.756 \pm 0.178	26.212 \pm 0.199	26.689 \pm 0.142	26.248 \pm 0.219	27.397 \pm 0.162	25.725 \pm 0.214
	Cluster-CP	26.027 \pm 0.325	25.415 \pm 0.289	26.288 \pm 0.407	25.712 \pm 0.315	26.969 \pm 0.305	25.532 \pm 0.350
	RC3P	18.129 \pm 0.003	17.082 \pm 0.002	17.784 \pm 0.003	17.465 \pm 0.003	18.111 \pm 0.002	17.167 \pm 0.004
HPS	CCP	24.633 \pm 0.212	24.467 \pm 0.149	24.379 \pm 0.152	24.472 \pm 0.167	25.449 \pm 0.196	23.885 \pm 0.159
	Cluster-CP	23.911 \pm 0.322	24.023 \pm 0.195	24.233 \pm 0.428	23.263 \pm 0.295	24.987 \pm 0.319	23.323 \pm 0.378
	RC3P	17.830 \pm 0.104	17.036 \pm 0.014	17.684 \pm 0.062	17.393 \pm 0.013	18.024 \pm 0.049	17.086 \pm 0.059
Food-101							
APS	CCP	27.022 \pm 0.192	30.900 \pm 0.170	30.943 \pm 0.119	35.912 \pm 0.105	27.415 \pm 0.194	36.776 \pm 0.132
	Cluster-CP	28.953 \pm 0.333	33.375 \pm 0.377	33.079 \pm 0.393	38.301 \pm 0.232	30.071 \pm 0.412	39.632 \pm 0.342
	RC3P	18.369 \pm 0.004	21.556 \pm 0.006	21.499 \pm 0.003	25.853 \pm 0.004	19.398 \pm 0.006	26.585 \pm 0.004
RAPS	CCP	27.022 \pm 0.192	30.900 \pm 0.170	30.966 \pm 0.125	35.940 \pm 0.111	27.439 \pm 0.203	36.802 \pm 0.138
	Cluster-CP	28.953 \pm 0.333	33.375 \pm 0.377	33.337 \pm 0.409	38.499 \pm 0.216	29.946 \pm 0.407	39.529 \pm 0.306
	RC3P	18.369 \pm 0.004	21.556 \pm 0.006	21.499 \pm 0.003	25.853 \pm 0.004	19.397 \pm 0.006	26.585 \pm 0.004
HPS	CCP	26.481 \pm 0.142	30.524 \pm 0.152	30.787 \pm 0.099	35.657 \pm 0.107	26.826 \pm 0.163	36.518 \pm 0.122
	Cluster-CP	29.347 \pm 0.288	33.806 \pm 0.513	33.407 \pm 0.345	38.956 \pm 0.242	29.606 \pm 0.436	39.880 \pm 0.318
	RC3P	18.337 \pm 0.004	21.558 \pm 0.006	21.477 \pm 0.003	25.853 \pm 0.005	19.396 \pm 0.008	26.584 \pm 0.003

- Average Prediction Set Size (APSS).

$$\text{APSS} := \sum_{c \in [K]} \frac{\mathbb{E}_{X_{\text{test}}} \mathbb{1}[y = c] \cdot |\hat{\mathcal{C}}_{1-\alpha}(x)|}{\mathbb{E}_{X_{\text{test}}} \mathbb{1}[y = c]} / K.$$

Table 3: **Balanced experiment on CIFAR-100, Places365, iNaturalist, ImageNet.** The models are pre-trained. UCR is controlled to ≤ 0.05 . RC3P significantly outperforms the best baseline with 32.826% reduction in APSS (\downarrow better) on average over $\min\{\text{CCP}, \text{cluster-CP}\}$.

Conformity Score	Measure	Methods	CIFAR-100	Places365	iNaturalist	ImageNet
APS	UCR	CCP	0.045 ± 0.008	0.012 ± 0.002	0.016 ± 0.001	0.036 ± 0.001
		Cluster-CP	0.023 ± 0.006	0.029 ± 0.003	0.026 ± 0.003	0.031 ± 0.002
		RC3P	0.006 ± 0.003	0.003 ± 0.001	0.008 ± 0.001	0.023 ± 0.001
	APSS	CCP	30.467 ± 0.307	19.698 ± 0.050	18.802 ± 0.023	101.993 ± 0.812
		Cluster-CP	32.628 ± 0.720	20.818 ± 0.173	23.467 ± 0.494	66.285 ± 1.433
		RC3P	12.551 ± 0.005	13.772 ± 0.005	12.736 ± 0.006	6.518 ± 0.001
RAPS	UCR	CCP	0.043 ± 0.006	0.013 ± 0.002	0.016 ± 0.020	0.038 ± 0.020
		Cluster-CP	0.016 ± 0.005	0.036 ± 0.002	0.027 ± 0.003	0.046 ± 0.004
		RC3P	0.002 ± 0.001	0.002 ± 0.001	0.006 ± 0.001	0.017 ± 0.001
	APSS	CCP	26.135 ± 0.308	15.694 ± 0.049	14.812 ± 0.042	37.748 ± 0.304
HPS	UCR	Cluster-CP	28.084 ± 0.609	16.750 ± 0.143	23.964 ± 0.419	16.155 ± 1.241
		RC3P	12.586 ± 0.002	14.192 ± 0.001	13.251 ± 0.001	6.560 ± 0.002
		CCP	0.034 ± 0.006	0.015 ± 0.002	0.018 ± 0.002	0.036 ± 0.002
	APSS	Cluster-CP	0.006 ± 0.003	0.029 ± 0.004	0.035 ± 0.002	0.039 ± 0.005
		RC3P	0.003 ± 0.002	0.002 ± 0.001	0.018 ± 0.002	0.006 ± 0.000

Note that coverage and predictive efficiency are two competing metrics in CP [20], e.g., achieving better coverage (resp. predictive efficiency) degenerates predictive efficiency (resp. coverage). Therefore, following the same strategy in [42], we choose to control their UCR as the same level that is close to 0 for a fair comparison over three class-conditional CP algorithms in terms of APSS. Meanwhile, to address the gap between population values and empirical ones (e.g., quantiles with $\tilde{O}(1/\sqrt{n_y})$ error bound, common to all CP methods [30, 1, 21], or class-wise top- k error ϵ_y^k with $\tilde{O}(1/\sqrt{n_y})$ error bound [12]), we uniformly add $g/\sqrt{n_y}$ (the same order with the standard concentration gap) to inflate the nominal coverage $1 - \alpha$ on each baseline and tune $g \in \{0.25, 0.5, 0.75, 1\}$ on the calibration dataset in terms of UCR. The detailed g values of each method are displayed in Appendix B.2. In addition, the actual achieved UCR values are shown in the complete results (see Appendix B.4, B.5, and B.6). For a complete evaluation, we add the experiments without controlling coverage on imbalanced datasets under the same setting and use the total under coverage gap (UCG) metric:

- *Under Coverage Gap (UCG).*

$$\text{UCG} := \sum_{c \in [K]} \max \left\{ 1 - \alpha - \frac{\mathbb{P}[Y \in \hat{\mathcal{C}}(X), \text{s.t. } Y=c]}{\mathbb{P}[Y=c]}, 0 \right\}.$$

Experiments with UCG metric evaluation are shown in the Appendix B.9.

5.2 Results and Discussion

We list empirical results in Table 2 for an overall comparison on four imbalanced datasets with $\rho = 0.5, 0.1$ using all three training distributions (EXP, POLY and MAJ) based on the considered APS, RAPS and HPS scoring functions. Complete experiment results under more values of ρ are in Appendix B. Results with APS, RAPS, and HPS scoring functions on balanced datasets are also summarized in Table 3. We make the following two key observations: (i) CCP, Cluster-CP, and RC3P can guarantee the class-conditional coverage (their UCRs are all close to 0) for all settings; (ii) RC3P significantly outperforms CCP and Cluster-CP in APSS on almost all imbalanced settings by reducing APSS with 24.47% on all four datasets and 32.63% on three datasets excluding CIFAR-10 compared with $\min\{\text{CCP}, \text{Cluster-CP}\}$ on average, while for balanced settings, RC3P still significantly outperforms the best baselines in terms of APSS with 32.826% APSS reduction.

To investigate the challenge of imbalanced data and more importantly, how RC3P significantly improves the APSS, we further conduct three careful experiments on imbalanced datasets. First, we report the histograms of class-conditional coverage and the corresponding histograms of prediction set size. This experiment verifies that RC3P derives significantly more class-conditional coverage above $1 - \alpha$ and thus reduces the prediction set size. Second, we visualize the normalized frequency of label rank included in prediction sets on testing datasets for all class-wise algorithms: CCP, Cluster-CP,

and RC3P. The normalized frequency is defined as: $\mathbb{P}(k) := \frac{\mathbb{E}_{X_{\text{test}}} \mathbb{1}[r_f(X_{\text{test}}, y) = k, y \in \hat{\mathcal{C}}(x)]}{\sum_{k=1}^K \mathbb{E}_{X_{\text{test}}} \mathbb{1}[r_f(X_{\text{test}}, y) = k, y \in \hat{\mathcal{C}}(x)]}$. Finally, we empirically verify the trade-off condition number $\{\sigma_y\}_{y=1}^K$ of Equation 6 on calibration dataset to reveal the underlying reason for RC3P producing smaller prediction sets over CCP with our standard training models (epoch = 200). We also evaluate $\{\sigma_y\}_{y=1}^K$ with less trained models (epoch = 50) on imbalanced datasets in Appendix B.10. Additionally, we also repeat all three experiments on balanced datasets (i.e., the histograms of class-conditional coverage and prediction set size, the normalized frequency of label rank included in prediction sets, and $\{\sigma_y\}_{y=1}^K$) in Appendix B.11. Below we discuss our experimental results and findings in detail.

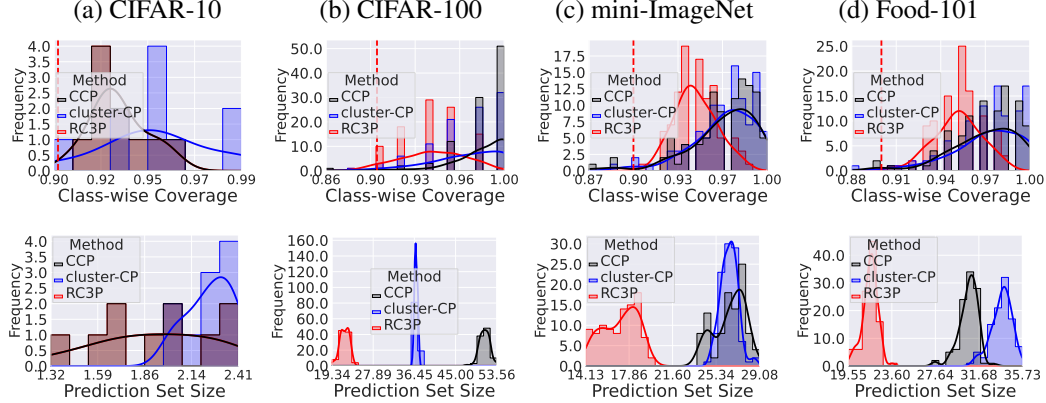


Figure 1: Class-conditional coverage (Top row) and prediction set size (Bottom row) achieved by CCP, Cluster-CP, and RC3P methods when $\alpha = 0.1$ and models are trained with 200 epochs on four imbalanced datasets with imbalance type EXP $\rho = 0.1$. We clarify that RC3P overlaps with CCP on CIFAR-10. It is clear that RC3P has more densely distributed class-conditional coverage above 0.9 (the target $1 - \alpha$ class-conditional coverage) than CCP and Cluster-CP with significantly smaller prediction sets on CIFAR-100, mini-ImageNet and Food-101.

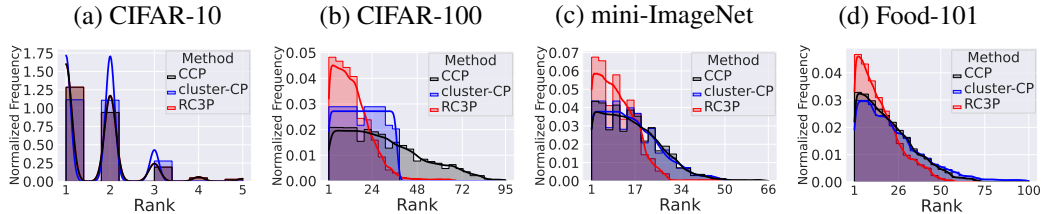


Figure 2: Visualization for the normalized frequency distribution of label ranks included in the prediction set of CCP, Cluster-CP, and RC3P with $\rho = 0.1$ for imbalance type EXP when $\alpha = 0.1$ and models are trained with 200 epochs. It is clear that the distribution of normalized frequency generated by RC3P tends to be lower compared to those produced by CCP and Cluster-CP. Furthermore, the probability density function tail for label ranks in the RC3P prediction set is notably shorter than that of other methods.

RC3P significantly outperforms CCP and Cluster-CP. First, it is clear from Table 6, 8, and 7, and 3 that RC3P, CCP, and Cluster-CP guarantee class-conditional coverage on all settings. This can also be observed by the first row of Fig 1, where the class-wise coverage bars of CCP and RC3P distribute on the right-hand side of the target probability $1 - \alpha$ (red dashed line). Second, RC3P outperforms CCP and Cluster-CP with 24.47% (four datasets) or 32.63% (excluding CIFAR-10) on imbalanced datasets and 32.63% on balanced datasets decrease in terms of average prediction set size for the same class-wise coverage. We also report the histograms of the corresponding prediction set sizes in the second row of Figure 1, which shows (i) RC3P has more concentrated class-wise coverage distribution than CCP and Cluster-CP; (ii) the distribution of prediction set sizes produced by RC3P is globally smaller than that produced by CCP and Cluster-CP, which is justified by a better trade-off number of $\{\sigma_y\}_{y=1}^K$ as shown in Figure 3. Note that the class-wise coverage and the corresponding prediction set sizes RC3P overlap with CCP on CIFAR-10 in Figure 1.

Visualization of normalized frequency. Figure 2 illustrates the normalized frequency distribution of label ranks included in the prediction sets across various testing datasets. It is evident that the

distribution of label ranks in the prediction set generated by RC3P tends to be lower compared to those produced by CCP and Cluster-CP. Furthermore, the probability density function tail for label ranks in the RC3P prediction set is notably shorter than that of other methods. This indicates that RC3P more effectively incorporates lower-ranked labels into prediction sets, as a result of its augmented rank calibration scheme.

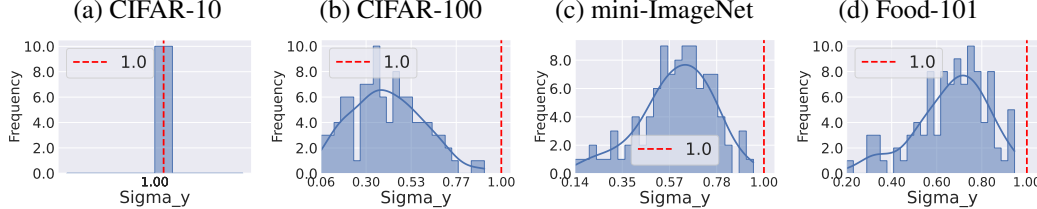


Figure 3: Verification of condition numbers $\{\sigma_y\}_{y=1}^K$ in Equation 6 with imbalance type EXP, $\rho = 0.1$ when $\alpha = 0.1$ and models are trained with 200 epochs. Vertical dashed lines represent the value 1, and we observe that all the condition numbers are smaller than 1. This verifies the validity of the condition for Lemma 4.2, and thus confirms that RC3P produces smaller prediction sets than CCP using calibration on both non-conformity scores and label ranks.

Verification of σ_y . Figure 3 verifies the validity of Equation (6) on testing datasets and confirms the optimized trade-off between the coverage with inflated quantile and the constraint with calibrated label rank leads to smaller prediction sets. It also confirms that the condition number $\{\sigma_y\}_{y=1}^K$ could be evaluated on calibration datasets without testing datasets and thus decreases the overall computation cost. We verify that $\sigma_y \leq 1$ for all settings and σ_y is much smaller than 1 on all datasets with large number of classes.

6 Summary

This paper studies a provable conformal prediction (CP) algorithm that aims to provide class-conditional coverage guarantee and to produce small prediction sets for classification tasks with many and/or imbalanced classes. Our proposed RC3P algorithm performs double-calibration, one over conformity score and one over label rank for each class separately, to achieve this goal. Our experiments clearly demonstrate the significant efficacy of RC3P over the baseline class-conditional CP algorithms on both balanced and imbalanced classification data settings.

Acknowledgments. This research was supported in part by United States Department of Agriculture (USDA) NIFA award No. 2021-67021-35344 (AgAID AI Institute) and by NSF CNS-2312125 grant.

References

- [1] Ghosh, S., Shi, Y., Belkhouja, T., Yan, Y., Doppa, J. & Jones, B. Probabilistically robust conformal prediction. *Uncertainty In Artificial Intelligence*. pp. 681-690 (2023)
- [2] Straitouri, E., Wang, L., Okati, N. & Rodriguez, M. Improving Expert Predictions with Conformal Prediction. *International Conference On Machine Learning (ICML)*. (2023)
- [3] Babbar, V., Bhatt, U. & Weller, A. On the utility of prediction sets in human-ai teams. *Proceedings Of The Thirty-First International Joint Conference On Artificial Intelligence (IJCAI-22)*. (2022)
- [4] Cui, Y., Jia, M., Lin, T., Song, Y. & Belongie, S. Class-balanced loss based on effective number of samples. *Proceedings Of The IEEE/CVF Conference On Computer Vision And Pattern Recognition*. pp. 9268-9277 (2019)
- [5] Cao, K., Wei, C., Gaidon, A., Arechiga, N. & Ma, T. Learning imbalanced datasets with label-distribution-aware margin loss. *Advances In Neural Information Processing Systems*. **32** (2019)
- [6] Krizhevsky, A., Hinton, G. & Others Learning multiple layers of features from tiny images. (Toronto, ON, Canada,2009)
- [7] Deng, J., Dong, W., Socher, R., Li, L., Li, K. & Fei-Fei, L. Imagenet: A large-scale hierarchical image database. *2009 IEEE Conference On Computer Vision And Pattern Recognition*. pp. 248-255 (2009)
- [8] He, K., Zhang, X., Ren, S. & Sun, J. Deep residual learning for image recognition. *Proceedings Of The IEEE Conference On Computer Vision And Pattern Recognition*. pp. 770-778 (2016)
- [9] Romano, Y., Sesia, M. & Candes, E. Classification with valid and adaptive coverage. *Advances In Neural Information Processing Systems*. **33** pp. 3581-3591 (2020)
- [10] Menon, A., Jayasumana, S., Rawat, A., Jain, H., Veit, A. & Kumar, S. Long-tail learning via logit adjustment. *ArXiv Preprint ArXiv:2007.07314*. (2020)
- [11] Vovk, V., Gammerman, A. & Shafer, G. Algorithmic learning in a random world. (Springer,2005)
- [12] Mohri, M., Rostamizadeh, A. & Talwalkar, A. Foundations of machine learning. (MIT press,2018)
- [13] Lei, J., Robins, J. & Wasserman, L. Distribution-free prediction sets. *Journal Of The American Statistical Association*. **108**, 278-287 (2013)
- [14] Vovk, V., Gammerman, A. & Saunders, C. Machine-learning applications of algorithmic randomness. (1999)
- [15] Shafer, G. & Vovk, V. A Tutorial on Conformal Prediction.. *Journal Of Machine Learning Research*. **9** (2008)
- [16] Gibbs, I. & Candes, E. Adaptive conformal inference under distribution shift. *Advances In Neural Information Processing Systems*. **34** pp. 1660-1672 (2021)
- [17] Tibshirani, R., Foygel Barber, R., Candes, E. & Ramdas, A. Conformal prediction under covariate shift. *Advances In Neural Information Processing Systems*. **32** (2019)
- [18] Sadinle, M., Lei, J. & Wasserman, L. Least ambiguous set-valued classifiers with bounded error levels. *Journal Of The American Statistical Association*. **114**, 223-234 (2019)
- [19] Guan, L. Localized conformal prediction: A generalized inference framework for conformal prediction. *Biometrika*. **110**, 33-50 (2023)
- [20] Angelopoulos, A., Bates, S., Malik, J. & Jordan, M. Uncertainty sets for image classifiers using conformal prediction. *ArXiv Preprint ArXiv:2009.14193*. (2020)
- [21] Angelopoulos, A. & Bates, S. A gentle introduction to conformal prediction and distribution-free uncertainty quantification. *ArXiv Preprint ArXiv:2107.07511*. (2021)
- [22] Chawla, N., Bowyer, K., Hall, L. & Kegelmeyer, W. SMOTE: synthetic minority over-sampling technique. *Journal Of Artificial Intelligence Research*. **16** pp. 321-357 (2002)
- [23] Tsai, C., Lin, W., Hu, Y. & Yao, G. Under-sampling class imbalanced datasets by combining clustering analysis and instance selection. *Information Sciences*. **477** pp. 47-54 (2019)

[24] Mohammed, R., Rawashdeh, J. & Abdullah, M. Machine learning with oversampling and undersampling techniques: overview study and experimental results. *2020 11th International Conference On Information And Communication Systems (ICICS)*. pp. 243-248 (2020)

[25] Krawczyk, B., Kozierski, M. & Woźniak, M. Radial-based oversampling for multiclass imbalanced data classification. *IEEE Transactions On Neural Networks And Learning Systems*. **31**, 2818-2831 (2019)

[26] Vuttipittayamongkol, P. & Elyan, E. Neighbourhood-based undersampling approach for handling imbalanced and overlapped data. *Information Sciences*. **509** pp. 47-70 (2020)

[27] Huang, C., Li, Y., Loy, C. & Tang, X. Deep imbalanced learning for face recognition and attribute prediction. *IEEE Transactions On Pattern Analysis And Machine Intelligence*. **42**, 2781-2794 (2019)

[28] Madabushi, H., Kochkina, E. & Castelle, M. Cost-sensitive BERT for generalisable sentence classification with imbalanced data. *ArXiv Preprint ArXiv:2003.11563*. (2020)

[29] Gottlieb, L., Kaufman, E. & Kontorovich, A. Apportioned margin approach for cost sensitive large margin classifiers. *Annals Of Mathematics And Artificial Intelligence*. **89**, 1215-1235 (2021)

[30] Vovk, V. Conditional validity of inductive conformal predictors. *Asian Conference On Machine Learning*. pp. 475-490 (2012)

[31] Vinyals, O., Blundell, C., Lillicrap, T., Wierstra, D. & Others Matching networks for one shot learning. *Advances In Neural Information Processing Systems*. **29** (2016)

[32] Bossard, L., Guillaumin, M. & Van Gool, L. Food-101—mining discriminative components with random forests. *Computer Vision—ECCV 2014: 13th European Conference, Zurich, Switzerland, September 6–12, 2014, Proceedings, Part VI* **13**. pp. 446-461 (2014)

[33] Ding, T., Angelopoulos, A., Bates, S., Jordan, M. & Tibshirani, R. Class-conditional conformal prediction with many classes. *Advances In Neural Information Processing Systems*. **36** (2024)

[34] Romano, Y., Patterson, E. & Candès, E. Conformalized quantile regression. *Advances In Neural Information Processing Systems*. **32** (2019)

[35] Huang, J., Xi, H., Zhang, L., Yao, H., Qiu, Y. & Wei, H. Conformal Prediction for Deep Classifier via Label Ranking. *ArXiv Preprint ArXiv:2310.06430*. (2023)

[36] Ghosh, S., Belkhouja, T., Yan, Y. & Doppa, J. Improving uncertainty quantification of deep classifiers via neighborhood conformal prediction: Novel algorithm and theoretical analysis. *Proceedings Of The AAAI Conference On Artificial Intelligence*. **37**, 7722-7730 (2023)

[37] Boström, H., Johansson, U. & Löfström, T. Mondrian conformal predictive distributions. *Conformal And Probabilistic Prediction And Applications*. pp. 24-38 (2021)

[38] Romano, Y., Barber, R., Sabatti, C. & Candès, E. With malice toward none: Assessing uncertainty via equalized coverage. *Harvard Data Science Review*. **2**, 4 (2020)

[39] Zaffran, M., Dieuleveut, A., Josse, J. & Romano, Y. Conformal prediction with missing values. *ArXiv Preprint ArXiv:2306.02732*. (2023)

[40] Fisch, A., Schuster, T., Jaakkola, T. & Barzilay, R. Few-shot conformal prediction with auxiliary tasks. *International Conference On Machine Learning*. pp. 3329-3339 (2021)

[41] Lu, C., Lemay, A., Chang, K., Höbel, K. & Kalpathy-Cramer, J. Fair conformal predictors for applications in medical imaging. *Proceedings Of The AAAI Conference On Artificial Intelligence*. **36**, 12008-12016 (2022)

[42] Fontana, M., Zeni, G. & Vantini, S. Conformal prediction: a unified review of theory and new challenges. *Bernoulli*. **29**, 1-23 (2023)

[43] Fisch, A., Schuster, T., Jaakkola, T. & Barzilay, R. Efficient conformal prediction via cascaded inference with expanded admission. *ArXiv Preprint ArXiv:2007.03114*. (2020)

[44] Vovk, V., Lindsay, D., Nouretdinov, I. & Gammerman, A. Mondrian confidence machine. *Technical Report*. (2003)

[45] Lei, J. & Wasserman, L. Distribution-free prediction bands for non-parametric regression. *Journal Of The Royal Statistical Society Series B: Statistical Methodology*. **76**, 71-96 (2014)

[46] Vovk, V., Fedorova, V., Nouretdinov, I. & Gammerman, A. Criteria of efficiency for conformal prediction. *Conformal And Probabilistic Prediction With Applications: 5th International Symposium, COPA 2016, Madrid, Spain, April 20-22, 2016, Proceedings* 5. pp. 23-39 (2016)

[47] Vazquez, J. & Facelli, J. Conformal prediction in clinical medical sciences. *Journal Of Healthcare Informatics Research*. **6**, 241-252 (2022)

[48] Lu, C., Angelopoulos, A. & Pomerantz, S. Improving trustworthiness of ai disease severity rating in medical imaging with ordinal conformal prediction sets. *International Conference On Medical Image Computing And Computer-Assisted Intervention*. pp. 545-554 (2022)

[49] Bates, S., Angelopoulos, A., Lei, L., Malik, J. & Jordan, M. Distribution-free, risk-controlling prediction sets. *Journal Of The ACM (JACM)*. **68**, 1-34 (2021)

[50] Angelopoulos, A., Bates, S., Fisch, A., Lei, L. & Schuster, T. Conformal risk control. *ArXiv Preprint ArXiv:2208.02814*. (2022)

[51] Cohen, K., Park, S., Simeone, O. & Shamai, S. Cross-Validation Conformal Risk Control. *ArXiv Preprint ArXiv:2401.11974*. (2024)

[52] Xu, Y., Guo, W. & Wei, Z. Conformal risk control for ordinal classification. *Uncertainty In Artificial Intelligence*. pp. 2346-2355 (2023)

[53] Lei, L. & Candès, E. Conformal inference of counterfactuals and individual treatment effects. *Journal Of The Royal Statistical Society Series B: Statistical Methodology*. **83**, 911-938 (2021)

[54] Barber, R., Candes, E., Ramdas, A. & Tibshirani, R. Conformal prediction beyond exchangeability. *The Annals Of Statistics*. **51**, 816-845 (2023)

[55] Gibbs, I. & Candès, E. Conformal inference for online prediction with arbitrary distribution shifts. *ArXiv Preprint ArXiv:2208.08401*. (2022)

[56] Jin, Y. & Candès, E. Model-free selective inference under covariate shift via weighted conformal p-values. (2023)

[57] Huang, K., Jin, Y., Candès, E. & Leskovec, J. Uncertainty Quantification over Graph with Conformalized Graph Neural Networks. *NeurIPS 2023*. (2023)

[58] Lei, J., G'Sell, M., Rinaldo, A., Tibshirani, R. & Wasserman, L. Distribution-free predictive inference for regression. *Journal Of The American Statistical Association*. **113**, 1094-1111 (2018)

[59] Bhatnagar, A., Wang, H., Xiong, C. & Bai, Y. Improved online conformal prediction via strongly adaptive online learning. *ArXiv Preprint ArXiv:2302.07869*. (2023)

[60] Feldman, S., Bates, S. & Romano, Y. Calibrated multiple-output quantile regression with representation learning. *Journal Of Machine Learning Research*. **24**, 1-48 (2023)

[61] Jöckel, L., Kläs, M., Groß, J. & Gerber, P. Conformal prediction and uncertainty wrapper: What statistical guarantees can you get for uncertainty quantification in machine learning?. *International Conference On Computer Safety, Reliability, And Security*. pp. 314-327 (2023)

[62] Sun, J., Jiang, Y., Qiu, J., Nobel, P., Kochenderfer, M. & Schwager, M. Conformal prediction for uncertainty-aware planning with diffusion dynamics model. *Advances In Neural Information Processing Systems*. **36** (2024)

[63] Dunn, R., Wasserman, L. & Ramdas, A. Distribution-free prediction sets with random effects. *ArXiv Preprint ArXiv:1809.07441*. (2018)

[64] Huang, J., Xi, H., Zhang, L., Yao, H., Qiu, Y., Wei, H. Conformal Prediction for Deep Classifier via Label Ranking. *ArXiv Preprint ArXiv:2310.06430*. (2024)

[65] Zhou, B., Lapedriza, A., Khosla, A., Oliva, A. & Torralba, A. Places: A 10 million image database for scene recognition. *IEEE Transactions On Pattern Analysis And Machine Intelligence*. **40**, 1452-1464 (2017)

[66] Van Horn, G., Mac Aodha, O., Song, Y., Cui, Y., Sun, C., Shepard, A., Adam, H., Perona, P. & Belongie, S. The inaturalist species classification and detection dataset. *Proceedings Of The IEEE Conference On Computer Vision And Pattern Recognition*. pp. 8769-8778 (2018)

[67] Russakovsky, O., Deng, J., Su, H., Krause, J., Satheesh, S., Ma, S., Huang, Z., Karpathy, A., Khosla, A., Bernstein, M. & Others Imagenet large scale visual recognition challenge. *International Journal Of Computer Vision*. **115** pp. 211-252 (2015)

- [68] Paszke, A., Gross, S., Massa, F., Lerer, A., Bradbury, J., Chanan, G., Killeen, T., Lin, Z., Gimelshein, N., Antiga, L. & Others Pytorch: An imperative style, high-performance deep learning library. *Advances In Neural Information Processing Systems*. **32** (2019)
- [69] Chen, T., Kornblith, S., Swersky, K., Norouzi, M. & Hinton, G. Big self-supervised models are strong semi-supervised learners. *Advances In Neural Information Processing Systems*. **33** pp. 22243-22255 (2020)

A Technical Proofs of Theoretical Results

A.1 Proof of Theorem 4.1

Theorem A.1. (Theorem 4.1 restated, class-conditional coverage of RC3P) Suppose that selecting $\hat{k}(y)$ values result in the class-wise top- k error $\epsilon_y^{\hat{k}(y)}$ for each class $y \in \mathcal{Y}$. For a target class-conditional coverage $1 - \alpha$, if we set $\hat{\alpha}_y$ and $\hat{k}(y)$ in RC3P (3) in the following ranges:

$$\hat{k}(y) \in \{k : \epsilon_y^k < \alpha\}, \quad 0 \leq \hat{\alpha}_y \leq \alpha - \epsilon_y^{\hat{k}(y)}, \quad (8)$$

then RC3P can achieve the class-conditional coverage for every $y \in \mathcal{Y}$:

$$\mathbb{P}_{(X,Y) \sim \mathcal{P}}\{Y \in \hat{\mathcal{C}}_{1-\alpha}^{\text{RC3P}}(X) | Y = y\} \geq 1 - \alpha.$$

Proof. (of Theorem 4.1)

Let $y \in \mathcal{Y}$ denote any class label. In this proof, we omit the superscript k in the top- k error notation ϵ_y^k for simplicity.

With the lower bound of the coverage on class y (Theorem 1 in [9]), we have

$$\begin{aligned} 1 - \hat{\alpha} &\leq \mathbb{P}\{Y_{\text{test}} \in \hat{\mathcal{C}}_{1-\hat{\alpha}}^{\text{CCP}}(X_{\text{test}}) | Y = y\} \\ &= \mathbb{P}\{V(X_{\text{test}}, Y_{\text{test}}) \leq \hat{Q}_{1-\hat{\alpha}}^{\text{class}}(y) | Y = y\} \\ &= \mathbb{P}\{V(X_{\text{test}}, Y_{\text{test}}) \leq \hat{Q}_{1-\hat{\alpha}}^{\text{class}}(y), r_f(X_{\text{test}}, Y_{\text{test}}) \leq \hat{k}(y) | Y = y\} \\ &\quad + \mathbb{P}\{V(X_{\text{test}}, Y_{\text{test}}) \leq \hat{Q}_{1-\hat{\alpha}}^{\text{class}}(y), r_f(X_{\text{test}}, Y_{\text{test}}) > \hat{k}(y) | Y = y\} \\ &\leq \mathbb{P}\{V(X_{\text{test}}, Y_{\text{test}}) \leq \hat{Q}_{1-\hat{\alpha}}^{\text{class}}(y), r_f(X_{\text{test}}, Y_{\text{test}}) \leq \hat{k}(y) | Y = y\} \\ &\quad + \underbrace{\mathbb{P}\{r_f(X_{\text{test}}, Y_{\text{test}}) > \hat{k}(y) | Y = y\}}_{\leq \epsilon_y^{\hat{k}(y)}} \\ &\leq \mathbb{P}\{Y_{\text{test}} \in \hat{\mathcal{C}}_{1-\hat{\alpha}}^{\text{RC3P}}(y) | Y = y\} + \epsilon_y^{\hat{k}(y)}. \end{aligned}$$

Re-arranging the above inequality, we have

$$\mathbb{P}\{Y_{\text{test}} \in \hat{\mathcal{C}}_{1-\hat{\alpha}}^{\text{RC3P}}(y) | Y = y\} \geq 1 - \hat{\alpha} - \epsilon_y^{\hat{k}(y)} \geq 1 - \alpha,$$

where the last inequality is due to $\hat{\alpha}_y \leq \alpha - \epsilon_y^{\hat{k}(y)}$. This implies that RC3P guarantees the class-conditional coverage on any class y . This completes the proof for Theorem 4.1. \square

A.2 Proof of Lemma 4.2

Theorem A.2. (Lemma 4.2 restated, improved predictive efficiency of RC3P) Let $\hat{\alpha}_y$ and $\hat{k}(y)$ satisfy Theorem 4.1. If the following inequality holds for any $y \in \mathcal{Y}$:

$$\mathbb{P}_{X_{\text{test}}}[V(X_{\text{test}}, y) \leq \hat{Q}_{1-\hat{\alpha}}^{\text{class}}(y), r_f(X_{\text{test}}, y) \leq \hat{k}(y)] \leq \mathbb{P}_{X_{\text{test}}}[V(X_{\text{test}}, y) \leq \hat{Q}_{1-\alpha}^{\text{class}}(y)], \quad (9)$$

then RC3P produces smaller expected prediction sets than CCP, i.e.,

$$\mathbb{E}_{X_{\text{test}}}[|\hat{\mathcal{C}}_{1-\hat{\alpha}}^{\text{RC3P}}(X_{\text{test}})|] \leq \mathbb{E}_{X_{\text{test}}}[|\hat{\mathcal{C}}_{1-\alpha}^{\text{CCP}}(X_{\text{test}})|].$$

Proof. (of Lemma 4.2)

The proof idea is to reduce the cardinality of the prediction set made by RC3P to that made by CCP

in expectation. Let $\sigma_y = \frac{\mathbb{P}_{X_{\text{test}}}[V(X_{\text{test}}, y) \leq \hat{Q}_{1-\hat{\alpha}}^{\text{class}}(y), r_f(X_{\text{test}}, y) \leq \hat{k}(y)]}{\mathbb{P}_{X_{\text{test}}}[V(X_{\text{test}}, y) \leq \hat{Q}_{1-\alpha}^{\text{class}}(y)]}$. According to the assumption in (9), we know that $\sigma_y \leq 1$, which will be used later.

We start with the expected prediction set size of RC3P and then derive its upper bound.

$$\begin{aligned}
\mathbb{E}_{X_{\text{test}}}[\|\widehat{\mathcal{C}}_{1-\hat{\alpha}}^{\text{RC3P}}(X_{\text{test}})\|] &= \mathbb{E}_{X_{\text{test}}}\left[\sum_{y \in \mathcal{Y}} \mathbb{1}\left[V(X_{\text{test}}, y) \leq \widehat{Q}_{1-\hat{\alpha}}^{\text{class}}(y), r_f(X_{\text{test}}, y) \leq \widehat{k}(y)\right]\right] \\
&= \sum_{y \in \mathcal{Y}} \mathbb{E}_{X_{\text{test}}}\left[\mathbb{1}[V(X_{\text{test}}, y) \leq \widehat{Q}_{1-\hat{\alpha}}^{\text{class}}(y), r_f(X_{\text{test}}, y) \leq \widehat{k}(y)]\right] \\
&= \sum_{y \in \mathcal{Y}} \mathbb{P}_{X_{\text{test}}}\left[V(X_{\text{test}}, y) \leq \widehat{Q}_{1-\hat{\alpha}}^{\text{class}}(y), r_f(X_{\text{test}}, y) \leq \widehat{k}(y)\right] \\
&\stackrel{(a)}{=} \sum_{y \in \mathcal{Y}} \sigma_y \cdot \mathbb{P}_{X_{\text{test}}}\left[V(X_{\text{test}}, y) \leq \widehat{Q}_{1-\alpha}^{\text{class}}(y)\right] \\
&\stackrel{(b)}{\leq} \sum_{y \in \mathcal{Y}} \mathbb{E}_{X_{\text{test}}}\left[\mathbb{1}[V(X_{\text{test}}, y) \leq \widehat{Q}_{1-\alpha}^{\text{class}}(y)]\right]
\end{aligned} \tag{10}$$

$$\begin{aligned}
&= \mathbb{E}_{X_{\text{test}}}\left[\sum_{y \in \mathcal{Y}} \mathbb{1}[V(X_{\text{test}}, y) \leq \widehat{Q}_{1-\alpha}^{\text{class}}(y)]\right] = \mathbb{E}_{X_{\text{test}}}[\|\widehat{\mathcal{C}}_{1-\alpha}^{\text{CCP}}(X_{\text{test}})\|],
\end{aligned} \tag{11}$$

where the equality (a) is due to the definitions of σ_y , and inequality (b) is due to the assumption

$$\sum_{y \in \mathcal{Y}} \sigma_y \cdot \mathbb{P}_{X_{\text{test}}}\left[V(X_{\text{test}}, y) \leq \widehat{Q}_{1-\alpha}^{\text{class}}(y)\right] \leq \sum_{y \in \mathcal{Y}} \mathbb{P}_{X_{\text{test}}}\left[V(X_{\text{test}}, y) \leq \widehat{Q}_{1-\alpha}^{\text{class}}(y)\right].$$

This shows that RC3P requires smaller prediction sets to guarantee the class-conditional coverage compared to CCP. \square

A.3 Proof of Theorem 4.3

Theorem A.3. (Theorem 4.3 restated, conditions of improved predictive efficiency for RC3P) Define $D = \mathbb{P}[r_f(X, y) \leq \widehat{k}(y) | Y \neq y]$, and $\bar{r}_f(X, y) = \lfloor \frac{r_f(X, y) + 1}{2} \rfloor$. Denote $B = \mathbb{P}[f(X)_{(\bar{r}_f(X, y))} \leq \widehat{Q}_{1-\alpha}^{\text{class}}(y) | Y \neq y]$ if V is APS, or $B = \mathbb{P}[f(X)_{(\bar{r}_f(X, y))} + \lambda \leq \widehat{Q}_{1-\alpha}^{\text{class}}(y) | Y \neq y]$ if V is RAPS. If $B - D \geq \frac{p_y}{1-p_y}(\alpha - \epsilon_y^{\widehat{k}(y)})$, then $\sigma_y \leq 1$.

Proof. (of Theorem 4.3)

Based on the different choices of scoring function, we first divide two scenarios:

(i): If $V(X, y)$ is the APS scoring function, since the APS score cumulatively sums the ordered prediction of $f(X)$: $V(X, y) = \sum_{l=1}^{r_f(X, y)} f(X)_{(l)}$, it is easy to verify that $V(X, y)$ is concave in terms of l . As a result, we have

$$\begin{aligned}
V(X, y) &= \frac{r_f(X, y)}{r_f(X, y)} \cdot \sum_{l=1}^{r_f(X, y)} f(X)_{(l)} \leq r_f(X, y) \cdot f(X)_{(\lfloor \sum_{l=1}^{r_f(X, y)} l / r_f(X, y) \rfloor)} = r_f(X, y) \cdot f(X)_{(\bar{r}_f(X, y))}, \\
\text{where } \bar{r}_f(X, y) &= \left\lfloor \frac{\sum_{l=1}^{r_f(X, y)} l}{r_f(X, y)} \right\rfloor = \lfloor (r_f(X, y) + 1) / 2 \rfloor.
\end{aligned}$$

Now we lower bound $\mathbb{P}_X[V(X, y) \leq \widehat{Q}_{1-\alpha}^{\text{class}}(y)]$ as follows.

$$\begin{aligned}
&\mathbb{P}_X[V(X, y) \leq \widehat{Q}_{1-\alpha}^{\text{class}}(y)] \\
&= \underbrace{\mathbb{P}_{XY}[Y = y]}_{=p_y} \cdot \underbrace{\mathbb{P}_X[V(X, y) \leq \widehat{Q}_{1-\alpha}^{\text{class}}(y) | Y = y]}_{\geq 1-\alpha} + \underbrace{\mathbb{P}_{XY}[Y \neq y]}_{=1-p_y} \cdot \underbrace{\mathbb{P}_X[V(X, y) \leq \widehat{Q}_{1-\alpha}^{\text{class}}(y) | Y \neq y]}_{\geq B} \\
&\geq p_y(1-\alpha) + (1-p_y)B + p_y(1-\epsilon_y^{\widehat{k}(y)}) + (1-p_y)D - p_y(1-\epsilon_y^{\widehat{k}(y)}) - (1-p_y)D \\
&\geq \mathbb{P}_X[r_f(X, y) \leq \widehat{k}(y)] - p_y(\alpha - \epsilon_y^{\widehat{k}(y)}) + (1-p_y)(B - D).
\end{aligned} \tag{12}$$

According to the assumption $B - D \geq \frac{p_y}{1-p_y}(\alpha - \epsilon_y^{\hat{k}(y)})$, we have

$$\mathbb{P}_X[r_f(X, y) \leq \hat{k}(y)] \leq \mathbb{P}_X[V(X, y) \leq \hat{Q}_{1-\alpha}^{\text{class}}(y)].$$

(ii): If $V(X, y)$ is the RAPS scoring function and $r_f(X, y) \leq k_{\text{reg}}$, then the RAPS scoring function could be rewritten as: $V(X, y) = \sum_{l=1}^{r_f(X, y)} f(X)_{(l)}$. As a result, we have:

$$\begin{aligned} V(X, y) &= \frac{r_f(X, y)}{r_f(X, y)} \cdot \sum_{l=1}^{r_f(X, y)} f(X)_{(l)} \\ &\leq r_f(X, y) \cdot f(X)_{(\lfloor \sum_{l=1}^{r_f(X, y)} l / r_f(X, y) \rfloor)} \\ &= r_f(X, y) \cdot f(X)_{(\bar{r}_f(X, y))} \\ &\leq r_f(X, y) \cdot (f(X)_{(\bar{r}_f(X, y))} + \lambda). \end{aligned}$$

If $r_f(X, y) > k_{\text{reg}}$, then the RAPS scoring function could be rewritten as: $V(X, y) = \sum_{l=1}^{r_f(X, y)} f(X)_{(l)} + \lambda(r_f(X, y) - k_{\text{reg}})$. As a result, we have

$$\begin{aligned} V(X, y) &= \frac{r_f(X, y)}{r_f(X, y)} \cdot \left(\sum_{l=1}^{r_f(X, y)} f(X)_{(l)} + \lambda(r_f(X, y) - k_{\text{reg}}) \right) \\ &\leq r_f(X, y) \cdot \left(f(X)_{(\bar{r}_f(X, y))} + \lambda \left(1 - \frac{k_{\text{reg}}}{r_f(X, y)} \right) \right) \\ &\leq r_f(X, y) \cdot (f(X)_{(\bar{r}_f(X, y))} + \lambda). \end{aligned}$$

Then, by applying the Inequality 12, we have:

$$\mathbb{P}_X[r_f(X, y) \leq \hat{k}(y)] \leq \mathbb{P}_X[V(X, y) \leq \hat{Q}_{1-\alpha}^{\text{class}}(y)].$$

This completes the proof for Theorem 4.3. \square

B Complete Experimental Results

B.1 Training Details

For CIFAR-10 and CIFAR-100, we train ResNet20 using LDAM loss function given in [5] with standard mini-batch stochastic gradient descent (SGD) using learning rate 0.1, momentum 0.9, and weight decay $2e-4$ for 200 epochs and 50 epochs. The batch size is 128. For experiments on mini-ImageNet, we use the same setting. For Food-101, the batch size is 256 and other parameters are kept the same. We reported our main results when models were trained in 200 epochs. Other results are reported in Appendix B.8 and Table 11.

We also evaluate the top-1 accuracy over the majority, medium, and minority groups of classes as the class-wise performance when 200 epochs. To show the variation of class-wise performance, we divide some classes with the largest number of data samples into the majority group, and the number of these classes is a quarter (25%) of the total number of classes. Similarly, we divide the classes with the smallest number of data into the minority group (25%) and the remaining classes as the medium group (50%). In the above table, we show the accuracy of three groups with three imbalance types and two imbalance ratios $\rho = 0.1, \rho = 0.5$ on four datasets.

The results are summarized in Table 4. As can be seen, the group-wise performance can vary significantly from high to very low. The class-imbalance setting is the case where the classifier does not perform very well in some classes.

B.2 Calibration Details

As mentioned in Section 5.1, we balanced split the validation set of CIFAR-10 and CIFAR-100, the number of calibration data is 5000. For mini-ImageNet, the number of calibration data is 15000. For

Table 4: Top-1 accuracy of minority, medium, and majority groups with three imbalance types and two imbalance ratios $\rho = 0.1, \rho = 0.5$ on four datasets. We could observe that the class-wise performance varies significantly over different classes.

Groups	EXP		POLY		MAJ	
	$\rho = 0.5$	$\rho = 0.1$	$\rho = 0.5$	$\rho = 0.1$	$\rho = 0.5$	$\rho = 0.1$
CIFAR-10						
Minority	0.913	0.961	0.932	0.901	0.940	0.927
Medium	0.872	0.822	0.867	0.847	0.848	0.75
Majority	0.949	0.832	0.933	0.948	0.914	0.795
CIFAR-100						
Minority	0.554	0.295	0.468	0.352	0.572	0.365
Medium	0.589	0.536	0.517	0.413	0.574	0.476
Majority	0.668	0.720	0.671	0.588	0.616	0.562
mini-ImageNet						
Minority	0.677	0.640	0.624	0.627	0.626	0.642
Medium	0.527	0.546	0.533	0.530	0.526	0.538
Majority	0.633	0.679	0.684	0.67	0.673	0.686
Food-101						
Minority	0.453	0.231	0.379	0.289	0.505	0.333
Medium	0.579	0.474	0.496	0.398	0.579	0.467
Majority	0.582	0.660	0.596	0.563	0.532	0.490

Food-101, the total number is 12625. To compute the mean and standard deviation for the overall performance, we repeat calibration experiments for 10 times. In our main results, We set $\alpha = 0.1$. We also report other experiment results of different α values, $\alpha = 0.05$ and $\alpha = 0.01$, in Appendix B.7, and Table 9 and 10.

The regularization parameter for RAPS scoring function is from the set $k_{reg} \in \{3, 5, 7\}$ and $\lambda \in \{0.001, 0.01, 0.1\}$ based on the empirical setting in `cluster-CP`. We select the combination of k_{reg} and λ for each experiment with the same imbalanced type and imbalanced ratio on the same dataset, where most of the APSS values of all methods are minimum.

The hyper-parameter g is selected from the set $\{0.25, 0.5, 0.75, 1.0\}$ to find the minimal g that CCP, `Cluster-CP`³, and RC3P achieve the target class-conditional coverage. We clarify that for each dataset and each class-conditional CP method, we use fixed g values. The detailed g values are displayed in Table 5. From Table 5, we could observe that the hyperparameter g for RC3P is always smaller than other methods, which means that comparing other class-wise CP algorithms, our algorithm needs the smallest inflation on $1 - \hat{\alpha}$ to achieve the target class-conditional coverage. This could also match the result of histograms of class-conditional coverage.

Table 5: Hyperparameter g choices for each class-conditional CP methods CCP, `Cluster-CP`, and RC3P on four datasets CIFAR-10, CIFAR-100, mini-ImageNet, and Food101. We could observe that all g values are in constant order to make a fair comparison. Meanwhile, the hyperparameter g for RC3P is always smaller than other methods.

Methods	Dataset			
	CIFAR-10	CIFAR-100	mini-ImageNet	FOOD-101
CCP	0.5	0.5	0.75	0.75
Cluster-CP	1.0	0.5	0.75	0.75
RC3P	0.5	0.25	0.5	0.5

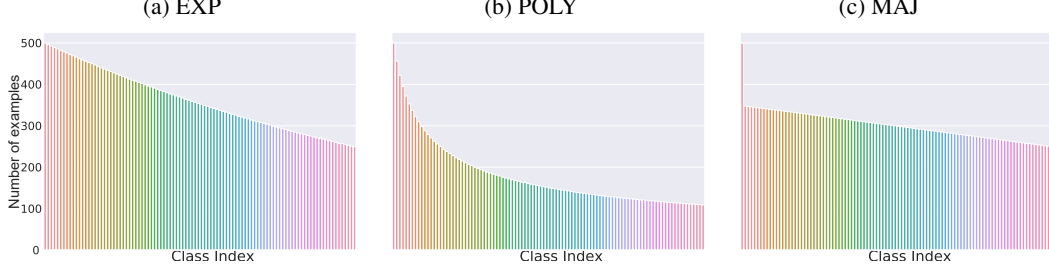


Figure 4: Illustrative examples of the different imbalanced distributions of the number of training examples per class index c on CIFAR-100

B.3 Illustration of Imbalanced Data

B.4 Comparison Experiments Using APS Score Function

Based on the results in Table 6, we make the following observations: (i) CCP, Cluster-CP, and RC3P can guarantee the class-conditional coverage; and (ii) RC3P significantly outperforms CCP and Cluster-CP on three datasets by producing smaller prediction sets.

Table 6: Results comparing CCP, Cluster-CP, and RC3P with ResNet-20 model and APS scoring function under different imbalance ratios $\rho = 0.5$ and $\rho = 0.1$ when $\alpha = 0.1$. We set UCR of RC3P the same as or better than that of CCP and Cluster-CP for a fair comparison of prediction set size. The APSS results show that RC3P significantly outperforms Cluster-CP in terms of the average prediction set size over all settings on CIFAR-100, mini-ImageNet, and Food-101.

Measure	Methods	EXP		POLY		MAJ	
		$\rho = 0.5$	$\rho = 0.1$	$\rho = 0.5$	$\rho = 0.1$	$\rho = 0.5$	$\rho = 0.1$
CIFAR-10							
UCR	CCP	0.050 \pm 0.016	0.100 \pm 0.020	0.100 \pm 0.032	0.050 \pm 0.021	0.070 \pm 0.014	0.040 \pm 0.015
	Cluster-CP	0.010 \pm 0.009	0.090 \pm 0.009	0.080 \pm 0.019	0.060 \pm 0.001	0.020 \pm 0.012	0.070 \pm 0.014
	RC3P	0.050 \pm 0.016	0.100 \pm 0.020	0.100 \pm 0.032	0.050 \pm 0.021	0.070 \pm 0.014	0.040 \pm 0.015
APSS	CCP	1.555 \pm 0.010	1.855 \pm 0.014	1.538 \pm 0.010	1.776 \pm 0.012	1.840 \pm 0.020	2.629 \pm 0.013
	Cluster-CP	1.714 \pm 0.018	2.162 \pm 0.015	1.706 \pm 0.014	1.928 \pm 0.013	1.948 \pm 0.023	3.220 \pm 0.020
	RC3P	1.555 \pm 0.010	1.855 \pm 0.014	1.538 \pm 0.010	1.776 \pm 0.012	1.840 \pm 0.020	2.629 \pm 0.013
CIFAR-100							
UCR	CCP	0.007 \pm 0.002	0.010 \pm 0.002	0.010 \pm 0.002	0.014 \pm 0.003	0.016 \pm 0.003	0.008 \pm 0.004
	Cluster-CP	0.012 \pm 0.002	0.016 \pm 0.004	0.020 \pm 0.003	0.004 \pm 0.002	0.016 \pm 0.003	0.019 \pm 0.005
	RC3P	0.005 \pm 0.002	0.011 \pm 0.002	0.009 \pm 0.003	0.015 \pm 0.003	0.008 \pm 0.002	0.008 \pm 0.004
APSS	CCP	44.224 \pm 0.341	50.969 \pm 0.345	49.889 \pm 0.353	64.343 \pm 0.237	44.194 \pm 0.514	64.642 \pm 0.535
	Cluster-CP	29.238 \pm 0.609	37.592 \pm 0.857	38.252 \pm 0.353	52.391 \pm 0.595	31.518 \pm 0.335	50.883 \pm 0.673
	RC3P	17.705 \pm 0.004	21.954 \pm 0.005	23.048 \pm 0.008	33.185 \pm 0.005	18.581 \pm 0.007	32.699 \pm 0.005
mini-ImageNet							
UCR	CCP	0.008 \pm 0.004	0.008 \pm 0.004	0.005 \pm 0.002	0.004 \pm 0.001	0.010 \pm 0.004	0.005 \pm 0.002
	Cluster-CP	0.014 \pm 0.004	0.012 \pm 0.004	0.011 \pm 0.003	0.014 \pm 0.003	0.008 \pm 0.002	0.010 \pm 0.003
	RC3P	0.000 \pm 0.000	0.001 \pm 0.001	0.000 \pm 0.000	0.000 \pm 0.000	0.000 \pm 0.000	0.000 \pm 0.000
APSS	CCP	26.676 \pm 0.171	26.111 \pm 0.194	26.626 \pm 0.133	26.159 \pm 0.208	27.313 \pm 0.154	25.629 \pm 0.207
	Cluster-CP	25.889 \pm 0.301	25.253 \pm 0.346	26.150 \pm 0.393	25.633 \pm 0.268	26.918 \pm 0.241	25.348 \pm 0.334
	RC3P	18.129 \pm 0.003	17.082 \pm 0.002	17.784 \pm 0.003	17.465 \pm 0.003	18.111 \pm 0.002	17.167 \pm 0.004
Food-101							
UCR	CCP	0.006 \pm 0.002	0.006 \pm 0.002	0.009 \pm 0.003	0.008 \pm 0.001	0.006 \pm 0.001	0.008 \pm 0.002
	Cluster-CP	0.003 \pm 0.002	0.009 \pm 0.003	0.004 \pm 0.001	0.009 \pm 0.002	0.011 \pm 0.003	0.011 \pm 0.002
	RC3P	0.000 \pm 0.000	0.000 \pm 0.000	0.000 \pm 0.000	0.001 \pm 0.001	0.000 \pm 0.000	0.000 \pm 0.000
APSS	CCP	27.022 \pm 0.192	30.900 \pm 0.170	30.943 \pm 0.119	35.912 \pm 0.105	27.415 \pm 0.194	36.776 \pm 0.132
	Cluster-CP	28.953 \pm 0.333	33.375 \pm 0.377	33.079 \pm 0.393	38.301 \pm 0.232	30.071 \pm 0.412	39.632 \pm 0.342
	RC3P	18.369 \pm 0.004	21.556 \pm 0.006	21.499 \pm 0.003	25.853 \pm 0.004	19.398 \pm 0.006	26.585 \pm 0.004

³<https://github.com/tiffanyding/class-conditional-conformal/tree/main>

B.5 Comparison Experiments Using RAPS Score Function

With the same model, evaluation metrics, and RAPS score function [20], we add the comparison experiments with CCP, and Cluster-CP on four datasets with different imbalanced types and imbalance ratio $\rho = 0.5$ and $\rho = 0.1$. The regularization parameter for RAPS scoring function is from the set $k_{reg} \in \{3, 5, 7\}$ and $\lambda \in \{0.001, 0.01, 0.1\}$. We select the combination of k_{reg} and λ for each experiment with the same imbalanced type and imbalanced ratio on the same dataset, where most of the APSS values of all methods are minimum. The overall performance is summarized in Table 7. We highlight that we also select the g from the set $g \in \{0.25, 0.5, 0.75, 1.0\}$ to find the minimal g that CCP, Cluster-CP, and RC3P approximately achieves the target class conditional coverage.

Based on the results in Table 7, we make the following observations: (i) CCP, Cluster-CP, and RC3P can guarantee the class-conditional coverage; and (ii) RC3P significantly outperforms CCP and Cluster-CP on three datasets by producing smaller prediction sets.

Table 7: Results comparing CCP, Cluster-CP, and RC3P with ResNet-20 model and the RAPS scoring function under different imbalance ratios $\rho = 0.5$ and $\rho = 0.1$ when $\alpha = 0.1$. The regularization parameter for RAPS scoring function is selected from the set $[3, 5, 7]$ and $[0.001, 0.01, 0.1]$. We select the best results for each element in the table. We set UCR of RC3P the same as or better than that of CCP and Cluster-CP for a fair comparison of prediction set size. The APSS results show that RC3P significantly outperforms CCP and Cluster-CP in terms of average prediction set size over all settings on CIFAR-100, mini-ImageNet, and Food-101.

Measure	Methods	EXP		POLY		MAJ	
		$\rho = 0.5$	$\rho = 0.1$	$\rho = 0.5$	$\rho = 0.1$	$\rho = 0.5$	$\rho = 0.1$
CIFAR-10							
UCR	CCP	0.050 \pm 0.016	0.010 \pm 0.020	0.100 \pm 0.028	0.050 \pm 0.021	0.070 \pm 0.014	0.040 \pm 0.015
	Cluster-CP	0.010 \pm 0.009	0.010 \pm 0.010	0.080 \pm 0.019	0.060 \pm 0.015	0.020 \pm 0.025	0.070 \pm 0.014
	RC3P	0.050 \pm 0.016	0.010 \pm 0.020	0.100 \pm 0.028	0.050 \pm 0.021	0.070 \pm 0.014	0.040 \pm 0.015
APSS	CCP	1.555 \pm 0.010	1.855 \pm 0.014	1.538 \pm 0.010	1.776 \pm 0.012	1.840 \pm 0.020	2.632 \pm 0.012
	Cluster-CP	1.714 \pm 0.018	2.162 \pm 0.015	1.706 \pm 0.014	1.929 \pm 0.013	1.787 \pm 0.019	2.968 \pm 0.024
	RC3P	1.555 \pm 0.010	1.855 \pm 0.014	1.538 \pm 0.010	1.776 \pm 0.012	1.840 \pm 0.020	2.632 \pm 0.012
CIFAR-100							
UCR	CCP	0.007 \pm 0.002	0.011 \pm 0.002	0.010 \pm 0.002	0.015 \pm 0.003	0.015 \pm 0.003	0.008 \pm 0.004
	Cluster-CP	0.012 \pm 0.002	0.017 \pm 0.004	0.019 \pm 0.004	0.034 \pm 0.005	0.008 \pm 0.003	0.018 \pm 0.006
	RC3P	0.005 \pm 0.002	0.011 \pm 0.002	0.009 \pm 0.003	0.015 \pm 0.003	0.015 \pm 0.003	0.008 \pm 0.004
APSS	CCP	44.250 \pm 0.342	50.970 \pm 0.345	49.886 \pm 0.353	64.332 \pm 0.236	48.343 \pm 0.353	64.663 \pm 0.535
	Cluster-CP	29.267 \pm 0.612	37.795 \pm 0.862	38.258 \pm 0.320	52.374 \pm 0.592	31.513 \pm 0.325	50.379 \pm 0.684
	RC3P	17.705 \pm 0.004	21.954 \pm 0.005	23.048 \pm 0.008	33.185 \pm 0.005	18.581 \pm 0.006	32.699 \pm 0.006
mini-ImageNet							
UCR	CCP	0.008 \pm 0.003	0.009 \pm 0.004	0.005 \pm 0.002	0.004 \pm 0.002	0.009 \pm 0.003	0.005 \pm 0.002
	Cluster-CP	0.006 \pm 0.002	0.013 \pm 0.005	0.009 \pm 0.003	0.016 \pm 0.001	0.007 \pm 0.002	0.009 \pm 0.004
	RC3P	0.000 \pm 0.000	0.001 \pm 0.001	0.000 \pm 0.000	0.000 \pm 0.000	0.000 \pm 0.000	0.000 \pm 0.000
APSS	CCP	26.756 \pm 0.178	26.212 \pm 0.199	26.689 \pm 0.142	26.248 \pm 0.219	27.397 \pm 0.162	25.725 \pm 0.214
	Cluster-CP	26.027 \pm 0.325	25.415 \pm 0.289	26.288 \pm 0.407	25.712 \pm 0.315	26.969 \pm 0.305	25.532 \pm 0.350
	RC3P	18.129 \pm 0.003	17.082 \pm 0.002	17.784 \pm 0.003	17.465 \pm 0.003	18.111 \pm 0.002	17.167 \pm 0.004
Food-101							
UCR	CCP	0.006 \pm 0.003	0.006 \pm 0.002	0.009 \pm 0.003	0.008 \pm 0.001	0.006 \pm 0.002	0.008 \pm 0.002
	Cluster-CP	0.004 \pm 0.003	0.012 \pm 0.004	0.006 \pm 0.002	0.006 \pm 0.003	0.011 \pm 0.003	0.014 \pm 0.004
	RC3P	0.000 \pm 0.000	0.000 \pm 0.000	0.000 \pm 0.000	0.001 \pm 0.001	0.000 \pm 0.000	0.000 \pm 0.000
APSS	CCP	27.022 \pm 0.192	30.900 \pm 0.170	30.966 \pm 0.125	35.940 \pm 0.111	27.439 \pm 0.203	36.802 \pm 0.138
	Cluster-CP	28.953 \pm 0.333	33.375 \pm 0.377	33.337 \pm 0.409	38.499 \pm 0.216	29.946 \pm 0.407	39.529 \pm 0.306
	RC3P	18.369 \pm 0.004	21.556 \pm 0.006	21.499 \pm 0.003	25.853 \pm 0.004	19.397 \pm 0.006	26.585 \pm 0.004

B.6 Comparison Experiments Using HPS Score Function

With the same model, evaluation metrics, and HPS score function [20], we add the comparison experiments with CCP, and Cluster-CP on four datasets with different imbalanced types and imbalance ratio $\rho = 0.5$ and $\rho = 0.1$. The overall performance is summarized in Table 8. We highlight that we also select the g from the set $g \in \{0.25, 0.5, 0.75, 1.0\}$ to find the minimal g that CCP, Cluster-CP, and RC3P approximately achieves the target class conditional coverage.

Based on the results in Table 8, we make the following observations: (i) CCP, Cluster-CP, and RC3P can guarantee the class-conditional coverage; and (ii) RC3P significantly outperforms CCP and Cluster-CP on three datasets by producing smaller prediction sets.

Table 8: Results comparing CCP, Cluster-CP, and RC3P with ResNet-20 model and the HPS scoring function under different imbalance ratios $\rho = 0.5$ and $\rho = 0.1$ when $\alpha = 0.1$. We set UCR of RC3P the same as or better than that of CCP and Cluster-CP for a fair comparison of prediction set size. RC3P significantly outperforms CCP and Cluster-CP with 20.91% (four datasets) or 27.88% (excluding CIFAR-10) reduction in APSS.

Measure	Methods	EXP		POLY		MAJ	
		$\rho = 0.5$	$\rho = 0.1$	$\rho = 0.5$	$\rho = 0.1$	$\rho = 0.5$	$\rho = 0.1$
CIFAR-10							
UCR	CCP	0.050 \pm 0.016	0.010 \pm 0.020	0.100 \pm 0.028	0.050 \pm 0.021	0.070 \pm 0.014	0.040 \pm 0.015
	Cluster-CP	0.010 \pm 0.009	0.010 \pm 0.010	0.080 \pm 0.019	0.060 \pm 0.015	0.020 \pm 0.025	0.070 \pm 0.014
	RC3P	0.050 \pm 0.016	0.010 \pm 0.020	0.100 \pm 0.028	0.050 \pm 0.021	0.070 \pm 0.014	0.040 \pm 0.015
APSS	CCP	1.144 \pm 0.005	1.324 \pm 0.007	1.137 \pm 0.003	1.243 \pm 0.005	1.272 \pm 0.008	1.936 \pm 0.010
	Cluster-CP	1.214 \pm 0.008	1.508 \pm 0.010	1.211 \pm 0.004	1.354 \pm 0.005	1.336 \pm 0.009	2.312 \pm 0.025
	RC3P	1.144 \pm 0.005	1.324 \pm 0.007	1.137 \pm 0.003	1.243 \pm 0.005	1.272 \pm 0.008	1.936 \pm 0.010
CIFAR-100							
UCR	CCP	0.007 \pm 0.002	0.011 \pm 0.002	0.010 \pm 0.002	0.015 \pm 0.003	0.015 \pm 0.003	0.008 \pm 0.004
	Cluster-CP	0.012 \pm 0.002	0.017 \pm 0.004	0.019 \pm 0.004	0.034 \pm 0.005	0.008 \pm 0.003	0.018 \pm 0.006
	RC3P	0.005 \pm 0.002	0.011 \pm 0.002	0.009 \pm 0.003	0.015 \pm 0.003	0.015 \pm 0.003	0.008 \pm 0.004
APSS	CCP	41.351 \pm 0.242	49.469 \pm 0.344	48.063 \pm 0.376	63.963 \pm 0.277	46.125 \pm 0.351	64.371 \pm 0.564
	Cluster-CP	27.566 \pm 0.555	35.528 \pm 0.979	36.101 \pm 0.565	51.333 \pm 0.776	29.323 \pm 0.363	50.519 \pm 0.679
	RC3P	20.363 \pm 0.006	25.212 \pm 0.010	25.908 \pm 0.007	36.951 \pm 0.018	21.149 \pm 0.006	35.606 \pm 0.005
mini-ImageNet							
UCR	CCP	0.008 \pm 0.003	0.009 \pm 0.004	0.005 \pm 0.002	0.004 \pm 0.002	0.009 \pm 0.003	0.005 \pm 0.002
	Cluster-CP	0.006 \pm 0.002	0.013 \pm 0.005	0.009 \pm 0.003	0.016 \pm 0.001	0.007 \pm 0.002	0.009 \pm 0.004
	RC3P	0.000 \pm 0.000	0.001 \pm 0.001	0.000 \pm 0.000	0.000 \pm 0.000	0.000 \pm 0.000	0.000 \pm 0.000
APSS	CCP	24.633 \pm 0.212	24.467 \pm 0.149	24.379 \pm 0.152	24.472 \pm 0.167	25.449 \pm 0.196	23.885 \pm 0.159
	Cluster-CP	23.911 \pm 0.322	24.023 \pm 0.195	24.233 \pm 0.428	23.263 \pm 0.295	24.987 \pm 0.319	23.323 \pm 0.378
	RC3P	17.830 \pm 0.104	17.036 \pm 0.014	17.684 \pm 0.062	17.393 \pm 0.013	18.024 \pm 0.049	17.086 \pm 0.059
Food-101							
UCR	CCP	0.006 \pm 0.003	0.006 \pm 0.002	0.009 \pm 0.003	0.008 \pm 0.001	0.006 \pm 0.002	0.008 \pm 0.002
	Cluster-CP	0.004 \pm 0.003	0.012 \pm 0.004	0.006 \pm 0.002	0.006 \pm 0.003	0.011 \pm 0.003	0.014 \pm 0.004
	RC3P	0.000 \pm 0.000	0.000 \pm 0.000	0.000 \pm 0.000	0.001 \pm 0.001	0.000 \pm 0.000	0.000 \pm 0.000
APSS	CCP	26.481 \pm 0.142	30.524 \pm 0.152	30.787 \pm 0.099	35.657 \pm 0.107	26.826 \pm 0.163	36.518 \pm 0.122
	Cluster-CP	29.347 \pm 0.288	33.806 \pm 0.513	33.407 \pm 0.345	38.956 \pm 0.242	29.606 \pm 0.436	39.880 \pm 0.318
	RC3P	18.337 \pm 0.004	21.558 \pm 0.006	21.477 \pm 0.003	25.853 \pm 0.005	19.396 \pm 0.008	26.584 \pm 0.003

B.7 Comparison Experiments with different target coverages

With the same model, evaluation metrics, and scoring functions, we add the comparison experiments with CCP, and Cluster-CP on four datasets with different imbalanced types and imbalance ratio $\rho = 0.5$ and $\rho = 0.1$ under the different α values. The overall performance is summarized in Table 9 and 10, with $\alpha = 0.05$ and $\alpha = 0.01$, respectively. We highlight that we also select the g from the set $g \in [0.15, 0.75]$ with 0.05 range to find the minimal g that CCP, Cluster-CP, and RC3P approximately achieves the target class conditional coverage.

Based on the results in Table 7, we make the following observations: (i) CCP, Cluster-CP, and RC3P can guarantee the class-conditional coverage; and (ii) RC3P significantly outperforms CCP and Cluster-CP on three datasets by producing smaller prediction sets.

Table 9: APSS results comparing CCP, Cluster-CP, and RC3P with ResNet-20 model under different imbalance ratio $\rho = 0.5$ and $\rho = 0.1$ where $\alpha = 0.05$. For a fair comparison of prediction set size, we set UCR of RC3P the same as or smaller (more restrictive) than that of CCP and Cluster-CP under 0.16 on CIFAR-10 and 0.03 on other datasets. The APSS results show that RC3P significantly outperforms CCP and Cluster-CP in terms of average prediction set size with 21.036% (four datasets) or 28.048% (excluding CIFAR-10) reduction in prediction size on average over $\min\{\text{CCP}, \text{cluster-CP}\}$.

Conformity Score	Methods	EXP		POLY		MAJ	
		$\rho = 0.5$	$\rho = 0.1$	$\rho = 0.5$	$\rho = 0.1$	$\rho = 0.5$	$\rho = 0.1$
CIFAR-10							
APS	CCP	2.861 ± 0.027	3.496 ± 0.037	2.744 ± 0.033	3.222 ± 0.018	3.269 ± 0.037	4.836 ± 0.035
	Cluster-CP	3.443 ± 0.041	4.551 ± 0.049	3.309 ± 0.037	4.012 ± 0.039	4.075 ± 0.069	5.958 ± 0.070
	RC3P	2.861 ± 0.027	3.496 ± 0.037	2.744 ± 0.033	3.222 ± 0.018	3.269 ± 0.037	4.836 ± 0.035
RAPS	CCP	2.833 ± 0.018	3.448 ± 0.036	2.774 ± 0.033	3.231 ± 0.021	3.301 ± 0.024	4.842 ± 0.037
	Cluster-CP	3.430 ± 0.044	4.389 ± 0.062	3.352 ± 0.035	3.876 ± 0.034	4.044 ± 0.055	5.959 ± 0.083
	RC3P	2.833 ± 0.018	3.448 ± 0.036	2.774 ± 0.033	3.231 ± 0.021	3.301 ± 0.024	4.842 ± 0.037
CIFAR-100							
APS	CCP	44.019 ± 0.295	51.004 ± 0.366	49.564 ± 0.315	64.314 ± 0.231	48.024 ± 0.386	64.941 ± 0.532
	Cluster-CP	39.641 ± 0.567	46.746 ± 0.147	47.654 ± 0.371	62.340 ± 0.404	37.634 ± 0.537	60.841 ± 0.391
	RC3P	32.128 ± 0.011	38.769 ± 0.006	39.930 ± 0.008	53.147 ± 0.010	34.361 ± 0.007	51.498 ± 0.009
RAPS	CCP	44.234 ± 0.341	50.950 ± 0.344	49.889 ± 0.355	64.339 ± 0.236	48.310 ± 0.353	64.628 ± 0.535
	Cluster-CP	39.212 ± 0.365	46.840 ± 0.186	49.094 ± 0.280	62.095 ± 0.278	41.596 ± 0.323	60.158 ± 0.536
	RC3P	32.135 ± 0.010	38.793 ± 0.007	39.871 ± 0.010	53.169 ± 0.009	34.380 ± 0.007	51.512 ± 0.008
mini-ImageNet							
APS	CCP	58.527 ± 0.445	57.527 ± 0.408	60.327 ± 0.520	56.581 ± 0.438	59.360 ± 0.430	56.636 ± 0.469
	Cluster-CP	47.613 ± 0.544	46.650 ± 0.699	47.117 ± 0.930	45.360 ± 0.582	59.002 ± 0.434	56.147 ± 0.456
	RC3P	32.046 ± 0.002	31.729 ± 0.003	31.718 ± 0.004	32.048 ± 0.003	32.909 ± 0.007	31.441 ± 0.004
RAPS	CCP	58.615 ± 0.428	57.626 ± 0.394	60.173 ± 0.527	56.702 ± 0.414	59.532 ± 0.430	56.903 ± 0.460
	Cluster-CP	47.427 ± 0.588	46.767 ± 0.724	47.302 ± 1.126	45.603 ± 0.639	59.408 ± 0.482	56.779 ± 0.486
	RC3P	32.040 ± 0.003	31.741 ± 0.003	31.752 ± 0.003	32.067 ± 0.002	32.914 ± 0.005	31.417 ± 0.005
Food-101							
APS	CCP	55.967 ± 0.464	60.374 ± 0.383	60.717 ± 0.596	65.698 ± 0.405	56.934 ± 0.446	66.654 ± 0.511
	Cluster-CP	48.699 ± 0.512	55.288 ± 0.815	54.063 ± 0.885	60.104 ± 0.608	48.894 ± 0.919	59.432 ± 0.754
	RC3P	31.224 ± 0.004	35.273 ± 0.007	35.364 ± 0.003	41.109 ± 0.005	31.661 ± 0.005	39.135 ± 0.003
RAPS	CCP	55.872 ± 0.465	60.764 ± 0.394	60.618 ± 0.579	65.681 ± 0.401	56.982 ± 0.447	66.615 ± 0.504
	Cluster-CP	48.371 ± 0.513	55.155 ± 0.775	53.813 ± 0.864	59.912 ± 0.530	49.259 ± 0.846	59.307 ± 0.648
	RC3P	31.229 ± 0.004	35.283 ± 0.006	35.379 ± 0.003	41.113 ± 0.005	31.631 ± 0.004	39.118 ± 0.003

Table 10: APSS results comparing CCP, Cluster-CP, and RC3P with ResNet-20 model under different imbalance ratio $\rho = 0.5$ and $\rho = 0.1$ where $\alpha = 0.01$. For a fair comparison of prediction set size, we set UCR of RC3P the same as or smaller (more restrictive) than that of CCP and Cluster-CP under 0.16 on CIFAR-10 and 0.03 on other datasets. The APSS results show that RC3P significantly outperforms CCP and Cluster-CP in terms of average prediction set size with 16.911% (four datasets) or 22.549% (excluding CIFAR-10) reduction in prediction size on average over $\min\{\text{CCP}, \text{cluster-CP}\}$.

Conformity Score	Methods	EXP		POLY		MAJ	
		$\rho = 0.5$	$\rho = 0.1$	$\rho = 0.5$	$\rho = 0.1$	$\rho = 0.5$	$\rho = 0.1$
CIFAR-10							
APS	CCP	7.250 \pm 0.164	7.387 \pm 0.116	7.173 \pm 0.079	7.596 \pm 0.109	7.392 \pm 0.128	8.864 \pm 0.108
	Cluster-CP	5.528 \pm 0.103	8.332 \pm 0.060	6.954 \pm 0.084	7.762 \pm 0.143	7.586 \pm 0.113	9.308 \pm 0.054
	RC3P	5.671 \pm 0.046	7.387 \pm 0.116	6.309 \pm 0.042	7.276 \pm 0.010	6.779 \pm 0.013	8.864 \pm 0.108
RAPS	CCP	7.294 \pm 0.160	7.458 \pm 0.101	7.067 \pm 0.106	7.597 \pm 0.096	7.547 \pm 0.134	8.884 \pm 0.106
	Cluster-CP	5.568 \pm 0.103	8.288 \pm 0.118	6.867 \pm 0.078	7.795 \pm 0.136	7.813 \pm 0.142	9.239 \pm 0.055
	RC3P	5.673 \pm 0.040	7.458 \pm 0.101	6.310 \pm 0.046	7.253 \pm 0.006	6.780 \pm 0.015	8.884 \pm 0.106
CIFAR-100							
APS	CCP	100.0 \pm 0.0	100.0 \pm 0.0	100.0 \pm 0.0	100.0 \pm 0.0	100.0 \pm 0.0	100.0 \pm 0.0
	Cluster-CP	65.523 \pm 0.495	69.063 \pm 0.512	67.012 \pm 0.739	81.997 \pm 0.390	100.0 \pm 0.0	100.0 \pm 0.0
	RC3P	55.621 \pm 0.007	63.039 \pm 0.007	60.258 \pm 0.005	74.927 \pm 0.007	100.0 \pm 0.0	100.0 \pm 0.0
RAPS	CCP	100.0 \pm 0.0	100.0 \pm 0.0	100.0 \pm 0.0	100.0 \pm 0.0	100.0 \pm 0.0	100.0 \pm 0.0
	Cluster-CP	65.584 \pm 0.508	69.373 \pm 0.466	66.313 \pm 0.745	82.043 \pm 0.439	100.0 \pm 0.0	100.0 \pm 0.0
	RC3P	55.632 \pm 0.008	63.021 \pm 0.006	60.205 \pm 0.006	74.885 \pm 0.006	100.0 \pm 0.0	100.0 \pm 0.0
mini-ImageNet							
APS	CCP	100.0 \pm 0.0					
	Cluster-CP	74.019 \pm 0.699	71.300 \pm 0.674	75.546 \pm 0.683	70.996 \pm 0.702	74.508 \pm 0.531	72.803 \pm 0.536
	RC3P	55.321 \pm 0.003	54.214 \pm 0.004	56.018 \pm 0.006	53.732 \pm 0.004	54.483 \pm 0.007	53.522 \pm 0.005
RAPS	CCP	100.0 \pm 0.0					
	Cluster-CP	73.893 \pm 0.734	70.638 \pm 0.657	75.546 \pm 0.683	71.098 \pm 0.706	74.675 \pm 0.578	73.345 \pm 0.474
	RC3P	55.270 \pm 0.003	54.184 \pm 0.003	56.733 \pm 0.006	53.736 \pm 0.004	55.304 \pm 0.004	53.532 \pm 0.005
Food-101							
APS	CCP	101.0 \pm 0.0					
	Cluster-CP	81.489 \pm 0.957	87.092 \pm 0.588	82.257 \pm 0.514	86.539 \pm 0.453	83.293 \pm 0.583	88.603 \pm 0.401
	RC3P	67.443 \pm 0.004	57.055 \pm 0.005	57.722 \pm 0.006	62.931 \pm 0.005	68.267 \pm 0.005	65.413 \pm 0.005
RAPS	CCP	101.0 \pm 0.0					
	Cluster-CP	81.505 \pm 0.955	87.103 \pm 0.587	82.272 \pm 0.513	86.517 \pm 0.455	83.367 \pm 0.635	88.604 \pm 0.404
	RC3P	67.444 \pm 0.004	57.069 \pm 0.005	57.722 \pm 0.006	62.938 \pm 0.004	68.266 \pm 0.005	65.457 \pm 0.006

B.8 Comparison Experiments when models are trained in different epochs

With the same loss function, training criteria, evaluation metrics, and two scoring functions, we add the comparison experiments with CCP, and Cluster-CP on four datasets with different imbalanced types and imbalance ratio $\rho = 0.5$ and $\rho = 0.1$ and $\alpha = 0.1$ when models are trained with 50 epochs. The overall performance is summarized in Table 11. We highlight that we also select the g from the set $g \in \{0.25, 0.5, 0.75, 1.0\}$ to find the minimal g that CCP, Cluster-CP, and RC3P approximately achieves the target class conditional coverage.

Based on the results in Table 7, we make the following observations: (i) CCP, Cluster-CP, and RC3P can guarantee the class-conditional coverage; and (ii) RC3P significantly outperforms CCP and Cluster-CP on three datasets by producing smaller prediction sets.

Table 11: APSS results comparing CCP, Cluster-CP, and RC3P with ResNet-20 model under different imbalance ratio $\rho = 0.5$ and $\rho = 0.1$ where $\alpha = 0.1$ and models are trained with 50 epochs. For a fair comparison of prediction set size, we set UCR of RC3P the same as or smaller (more restrictive) than that of CCP and Cluster-CP under 0.16 on CIFAR-10 and 0.03 on other datasets. The APSS results show that RC3P significantly outperforms CCP and Cluster-CP in terms of average prediction set size with 21.441% (four datasets) or 28.588% (excluding CIFAR-10) reduction in prediction size on average over $\min\{\text{CCP, cluster-CP}\}$.

Conformity Score	Methods	EXP		POLY		MAJ	
		$\rho = 0.5$	$\rho = 0.1$	$\rho = 0.5$	$\rho = 0.1$	$\rho = 0.5$	$\rho = 0.1$
CIFAR-10							
APS	CCP	2.420 ± 0.019	2.661 ± 0.015	2.399 ± 0.013	2.519 ± 0.022	2.651 ± 0.031	4.053 ± 0.021
	Cluster-CP	4.006 ± 0.019	3.574 ± 0.023	3.144 ± 0.020	2.994 ± 0.029	3.698 ± 0.044	5.290 ± 0.016
	RC3P	2.420 ± 0.019	2.661 ± 0.015	2.399 ± 0.013	2.519 ± 0.022	2.651 ± 0.031	4.053 ± 0.021
RAPS	CCP	2.096 ± 0.014	2.533 ± 0.019	2.383 ± 0.026	2.247 ± 0.017	2.232 ± 0.019	3.233 ± 0.021
	Cluster-CP	2.625 ± 0.017	3.099 ± 0.021	2.840 ± 0.043	2.843 ± 0.026	2.770 ± 0.025	3.961 ± 0.029
	RC3P	2.096 ± 0.014	2.533 ± 0.019	2.383 ± 0.026	2.247 ± 0.017	2.232 ± 0.019	3.233 ± 0.021
CIFAR-100							
APS	CCP	52.655 ± 0.473	52.832 ± 0.308	54.523 ± 0.441	61.768 ± 0.195	52.119 ± 0.197	58.333 ± 0.299
	Cluster-CP	42.990 ± 0.655	43.275 ± 0.833	44.114 ± 0.458	58.226 ± 0.627	39.841 ± 0.836	53.409 ± 0.520
	RC3P	24.872 ± 0.008	25.107 ± 0.006	27.757 ± 0.004	35.733 ± 0.010	24.496 ± 0.010	32.172 ± 0.007
RAPS	CCP	52.662 ± 0.473	52.841 ± 0.307	54.528 ± 0.442	61.766 ± 0.195	52.129 ± 0.197	58.331 ± 0.299
	Cluster-CP	43.024 ± 0.648	43.277 ± 0.839	44.120 ± 0.458	58.212 ± 0.629	39.864 ± 0.845	53.402 ± 0.518
	RC3P	24.872 ± 0.008	25.107 ± 0.006	27.757 ± 0.004	35.733 ± 0.010	24.496 ± 0.010	32.173 ± 0.007
mini-ImageNet							
APS	CCP	42.404 ± 0.213	41.154 ± 0.191	38.433 ± 0.248	36.363 ± 0.228	36.047 ± 0.191	37.600 ± 0.208
	Cluster-CP	42.006 ± 0.430	41.101 ± 0.224	39.016 ± 0.273	36.046 ± 0.467	35.721 ± 0.355	37.975 ± 0.559
	RC3P	32.022 ± 0.005	31.909 ± 0.004	28.460 ± 0.003	26.383 ± 0.003	26.128 ± 0.005	28.127 ± 0.005
RAPS	CCP	42.516 ± 0.215	37.552 ± 0.192	38.730 ± 0.218	37.800 ± 0.186	36.595 ± 0.244	36.057 ± 0.206
	Cluster-CP	42.231 ± 0.386	37.448 ± 0.332	38.602 ± 0.327	37.939 ± 0.309	36.351 ± 0.308	35.724 ± 0.242
	RC3P	32.022 ± 0.005	29.114 ± 0.004	28.197 ± 0.006	27.626 ± 0.004	25.853 ± 0.003	25.948 ± 0.003
Food-101							
APS	CCP	41.669 ± 0.118	51.395 ± 0.247	44.261 ± 0.165	58.816 ± 0.162	52.672 ± 0.169	57.312 ± 0.162
	Cluster-CP	44.883 ± 0.336	54.684 ± 0.475	47.794 ± 0.420	60.727 ± 0.178	56.100 ± 0.257	60.200 ± 0.543
	RC3P	31.987 ± 0.005	36.118 ± 0.016	34.576 ± 0.006	49.299 ± 0.005	43.680 ± 0.005	47.649 ± 0.006
RAPS	CCP	41.803 ± 0.157	48.548 ± 0.107	44.288 ± 0.165	56.592 ± 0.165	47.264 ± 0.120	56.666 ± 0.160
	Cluster-CP	44.810 ± 0.565	51.091 ± 0.375	47.861 ± 0.428	59.262 ± 0.306	50.211 ± 0.474	60.183 ± 0.507
	RC3P	34.240 ± 0.115	36.425 ± 0.024	34.576 ± 0.006	46.074 ± 0.004	37.055 ± 0.006	48.012 ± 0.076

B.9 Comparison Experiments with UCG metrics

We add the experiments without controlling coverage on imbalanced datasets under the same setting as the main paper. We then use the total under coverage gap (UCG, ↓ better) between class conditional coverage and target coverage $1 - \alpha$ of all under covered classes. We choose UCG as the fine-grained metric to differentiate the coverage performance in our experiment setting. Conditioned on similar APSS of all methods, RC3P significantly outperforms the best baselines with 35.18% (four datasets) or 46.91% (excluding CIFAR-10) reduction in UCG on average.

Table 12: UCG and APSS results comparing CCP, Cluster-CP, and RC3P with ResNet-20 model trained with 200 epochs under different imbalance types with imbalance ratio $\rho = 0.1$, where the coverage of each method are not aligned. The APSS results show that RC3P outperforms CCP and Cluster-CP in terms of average prediction set size with 1.64%(four datasets) or 2.19% (excluding CIFAR-10) reduction in prediction size on average over $\min\{\text{CCP}, \text{cluster-CP}\}$. The UCG results show that RC3P achieve the similar class conditional coverage as CCP and Cluster-CP in terms of with 35.18%(four datasets) or 46.91% (excluding CIFAR-10) increment in the proportion of under coverage classes on average over $\min\{\text{CCP}, \text{cluster-CP}\}$.

Conformity Score	Methods	EXP		POLY		MAJ	
		UCG	APSS	UCG	APSS	UCG	APSS
CIFAR-10							
APS	CCP	0.014 ± 0.000	1.573 ± 0.009	0.032 ± 0.000	1.494 ± 0.015	0.068 ± 0.000	2.175 ± 0.019
	Cluster-CP	0.160 ± 0.000	1.438 ± 0.012	0.124 ± 0.000	1.280 ± 0.007	0.144 ± 0.000	2.079 ± 0.023
	RC3P	0.014 ± 0.000	1.573 ± 0.009	0.032 ± 0.043	1.494 ± 0.015	0.068 ± 0.031	2.175 ± 0.019
RAPS	CCP	0.014 ± 0.000	1.573 ± 0.009	0.032 ± 0.000	1.494 ± 0.015	0.070 ± 0.000	2.179 ± 0.019
	Cluster-CP	0.160 ± 0.000	1.438 ± 0.012	0.124 ± 0.000	1.280 ± 0.007	0.144 ± 0.000	2.079 ± 0.023
	RC3P	0.014 ± 0.050	1.573 ± 0.009	0.032 ± 0.000	1.494 ± 0.015	0.070 ± 0.000	2.179 ± 0.019
CIFAR-100							
APS	CCP	1.920 ± 0.000	16.721 ± 0.174	2.000 ± 0.000	26.831 ± 0.150	2.400 ± 0.000	26.211 ± 0.216
	Cluster-CP	1.500 ± 0.000	15.657 ± 0.417	2.580 ± 0.000	26.709 ± 0.422	2.660 ± 0.000	25.145 ± 0.385
	RC3P	0.840 ± 0.000	14.642 ± 0.005	1.200 ± 0.000	24.480 ± 0.004	1.460 ± 0.000	23.332 ± 0.006
RAPS	CCP	1.920 ± 0.000	16.724 ± 0.174	2.020 ± 0.000	26.817 ± 0.150	2.400 ± 0.007	26.199 ± 0.216
	Cluster-CP	1.500 ± 0.000	15.767 ± 0.410	2.760 ± 0.000	26.712 ± 0.512	2.480 ± 0.000	25.153 ± 0.250
	RC3P	0.840 ± 0.000	14.642 ± 0.005	1.200 ± 0.000	24.480 ± 0.004	1.460 ± 0.000	23.332 ± 0.006
mini-ImageNet							
APS	CCP	1.486 ± 0.000	10.525 ± 0.093	1.620 ± 0.000	11.188 ± 0.094	1.280 ± 0.000	10.642 ± 0.055
	Cluster-CP	1.313 ± 0.000	11.133 ± 0.118	1.453 ± 0.000	11.547 ± 0.129	1.640 ± 0.000	11.186 ± 0.151
	RC3P	0.713 ± 0.000	10.360 ± 0.042	0.653 ± 0.000	11.089 ± 0.052	0.600 ± 0.000	10.545 ± 0.029
RAPS	CCP	1.526 ± 0.000	10.570 ± 0.093	1.620 ± 0.000	11.250 ± 0.095	1.293 ± 0.000	10.702 ± 0.055
	Cluster-CP	1.480 ± 0.000	11.192 ± 0.123	1.513 ± 0.000	11.704 ± 0.124	1.586 ± 0.000	11.231 ± 0.156
	RC3P	0.713 ± 0.000	10.377 ± 0.035	0.653 ± 0.000	11.126 ± 0.046	0.600 ± 0.000	10.571 ± 0.021
Food-101							
APS	CCP	1.176 ± 0.000	14.019 ± 0.064	1.208 ± 0.000	17.288 ± 0.075	1.748 ± 0.000	17.663 ± 0.076
	Cluster-CP	1.296 ± 0.000	13.998 ± 0.107	1.704 ± 0.000	17.300 ± 0.183	2.148 ± 0.000	17.410 ± 0.130
	RC3P	0.556 ± 0.000	13.564 ± 0.003	0.664 ± 0.000	16.608 ± 0.006	0.924 ± 0.000	16.890 ± 0.005
RAPS	CCP	1.160 ± 0.000	14.019 ± 0.064	1.208 ± 0.000	17.301 ± 0.075	1.764 ± 0.000	17.679 ± 0.076
	Cluster-CP	1.308 ± 0.000	14.080 ± 0.113	1.804 ± 0.000	17.370 ± 0.198	1.944 ± 0.000	17.488 ± 0.138
	RC3P	0.556 ± 0.000	13.564 ± 0.003	0.664 ± 0.000	16.608 ± 0.006	0.924 ± 0.000	16.890 ± 0.005

B.10 Complete Experiment Results on Imbalanced Datasets

In this subsection, we report complete experimental results over four imbalanced datasets, three decaying types, and five imbalance ratios when epoch = 200 and $\alpha = 0.1$. Specifically, Table 13, 14, 15 report results on CIFAR-10 with three decaying types. Table 16, 17, 18 report results on CIFAR-100 with three decaying types. Table 19, 20, 21 report results on mini-ImageNet with three decaying types. Table 22, 23, 24 report results on Food-101 with three decaying types.

Figure 5, Figure 6, Figure 7, Figure 8 and Figure 9 show the class-conditional coverage and the corresponding prediction set sizes on EXP $\rho = 0.5$, POLY $\rho = 0.1$, POLY $\rho = 0.5$, MAJ $\rho = 0.1$, MAJ $\rho = 0.5$, respectively. This result on EXP $\rho = 0.1$ is in Figure 1.

Figure 10, Figure 11, Figure 12, Figure 13 and Figure 14 illustrates the normalized frequency distribution of label ranks included in the prediction sets on EXP $\rho = 0.5$, POLY $\rho = 0.1$, POLY $\rho = 0.5$, MAJ $\rho = 0.1$, MAJ $\rho = 0.5$, respectively. This result on EXP $\rho = 0.1$ is in Figure 2. It is evident that the distribution of label ranks in the prediction set generated by RC3P tends to be lower compared to those produced by CCP and Cluster-CP. Furthermore, the probability density function tail for label ranks in the RC3P prediction set is notably shorter than that of other methods. This indicates that RC3P more effectively incorporates lower-ranked labels into prediction sets, as a result of its augmented rank calibration scheme.

Figure 15, Figure 16, Figure 17, Figure 18 and Figure 19 verify the condition numbers σ_y when models are fully trained (epoch = 200) on EXP $\rho = 0.5$, POLY $\rho = 0.1$, POLY $\rho = 0.5$, MAJ $\rho = 0.1$, MAJ $\rho = 0.5$, respectively. This result on EXP $\rho = 0.1$ is in Figure 3. We also evaluate the condition numbers σ_y when models are lessly trained (epoch = 50) and $\alpha = 0.1$ on EXP $\rho = 0.5$, EXP $\rho = 0.1$, POLY $\rho = 0.1$, POLY $\rho = 0.5$, MAJ $\rho = 0.1$, MAJ $\rho = 0.5$, respectively. These results are shown from Figure 21 to Figure 25. These results verify the validity of Lemma 4.2 and Equation 6 and confirm that the optimized trade-off between the coverage with inflated quantile and the constraint with calibrated rank leads to smaller prediction sets. They also show a stronger condition ($\sigma_y \leq 1$ for all y) than the weighted aggregation condition in (5). They also confirm that the condition number $\{\sigma_y\}_{y=1}^C$ could be evaluated on calibration datasets without testing datasets and thus decreases the computation cost. We notice that RC3P degenerates to CCP on CIFAR-10, so $\sigma_y = 1$ for all y and there is no trade-off. On the other three datasets, we observe significant conditions for the optimized trade-off in RC3P.

Table 13: Results comparing CCP, cluster-CP, and RC3P with ResNet-20 model under different imbalance ratio $\rho = 0.5$, $\rho = 0.4$, $\rho = 0.2$, and $\rho = 0.1$ with imbalance type EXP and two scoring functions, APS and RAPS, on dataset CIFAR-10. We set UCR of RC3P the same as or better than that of CCP and Cluster-CP for a fair comparison of prediction set size.

Scoring function	Measure	Methods	EXP				
			$\rho = 0.5$	$\rho = 0.4$	$\rho = 0.3$	$\rho = 0.2$	$\rho = 0.1$
APS	UCR	CCP	0.050 \pm 0.016	0.06 \pm 0.021	0.050 \pm 0.016	0.050 \pm 0.021	0.100 \pm 0.020
		Cluster-CP	0.010 \pm 0.009	0.050 \pm 0.021	0.0 \pm 0.0	0.030 \pm 0.015	0.090 \pm 0.009
		RC3P	0.050 \pm 0.016	0.06 \pm 0.021	0.050 \pm 0.016	0.050 \pm 0.021	0.100 \pm 0.020
	APSS	CCP	1.555 \pm 0.010	1.595 \pm 0.013	1.643 \pm 0.008	1.676 \pm 0.014	1.855 \pm 0.014
		Cluster-CP	1.714 \pm 0.018	1.745 \pm 0.018	1.825 \pm 0.014	1.901 \pm 0.022	2.162 \pm 0.015
		RC3P	1.555 \pm 0.010	1.595 \pm 0.013	1.643 \pm 0.008	1.676 \pm 0.014	1.855 \pm 0.014
RAPS	UCR	CCP	0.050 \pm 0.016	0.060 \pm 0.021	0.050 \pm 0.016	0.050 \pm 0.021	0.010 \pm 0.020
		Cluster-CP	0.010 \pm 0.010	0.050 \pm 0.021	0.000 \pm 0.000	0.030 \pm 0.014	0.010 \pm 0.010
		RC3P	0.050 \pm 0.016	0.060 \pm 0.021	0.050 \pm 0.016	0.050 \pm 0.021	0.010 \pm 0.020
	APSS	CCP	1.555 \pm 0.010	1.595 \pm 0.013	1.643 \pm 0.008	1.676 \pm 0.014	1.855 \pm 0.014
		Cluster-CP	1.714 \pm 0.018	1.745 \pm 0.018	1.825 \pm 0.014	1.901 \pm 0.022	2.162 \pm 0.015
		RC3P	1.555 \pm 0.010	1.595 \pm 0.013	1.643 \pm 0.008	1.676 \pm 0.014	1.855 \pm 0.014

Table 14: Results comparing CCP, cluster-CP, and RC3P with ResNet-20 model under different imbalance ratio $\rho = 0.5, \rho = 0.4, \rho = 0.2$, and $\rho = 0.1$ with imbalance type POLY and two scoring functions, APS and RAPS, on dataset CIFAR-10. We set UCR of RC3P the same as or better than that of CCP and Cluster-CP for a fair comparison of prediction set size.

Scoring function	Measure	Methods	POLY				
			$\rho = 0.5$	$\rho = 0.4$	$\rho = 0.3$	$\rho = 0.2$	$\rho = 0.1$
APS	UCR	CCP	0.100 \pm 0.028	0.060 \pm 0.026	0.060 \pm 0.015	0.050 \pm 0.021	0.050 \pm 0.021
		Cluster-CP	0.080 \pm 0.019	0.050 \pm 0.021	0.050 \pm 0.025	0.050 \pm 0.016	0.060 \pm 0.015
		RC3P	0.100 \pm 0.028	0.060 \pm 0.026	0.060 \pm 0.015	0.050 \pm 0.021	0.050 \pm 0.021
	APSS	CCP	1.538 \pm 0.010	1.546 \pm 0.011	1.580 \pm 0.014	1.627 \pm 0.011	1.776 \pm 0.012
		Cluster-CP	1.706 \pm 0.014	1.718 \pm 0.014	1.758 \pm 0.016	1.783 \pm 0.016	1.928 \pm 0.013
		RC3P	1.538 \pm 0.010	1.546 \pm 0.011	1.580 \pm 0.014	1.627 \pm 0.011	1.776 \pm 0.012
RAPS	UCR	CCP	0.100 \pm 0.028	0.060 \pm 0.025	0.060 \pm 0.016	0.050 \pm 0.021	0.050 \pm 0.021
		Cluster-CP	0.080 \pm 0.019	0.050 \pm 0.021	0.050 \pm 0.025	0.050 \pm 0.016	0.060 \pm 0.015
		RC3P	0.100 \pm 0.028	0.060 \pm 0.025	0.060 \pm 0.016	0.050 \pm 0.021	0.050 \pm 0.021
	APSS	CCP	1.538 \pm 0.010	1.546 \pm 0.011	1.581 \pm 0.014	1.627 \pm 0.011	1.776 \pm 0.012
		Cluster-CP	1.706 \pm 0.014	1.719 \pm 0.014	1.759 \pm 0.016	1.783 \pm 0.016	1.929 \pm 0.013
		RC3P	1.538 \pm 0.010	1.546 \pm 0.011	1.581 \pm 0.014	1.627 \pm 0.011	1.776 \pm 0.012

Table 15: Results comparing CCP, cluster-CP, and RC3P with ResNet-20 model under different imbalance ratio $\rho = 0.5, \rho = 0.4, \rho = 0.2$, and $\rho = 0.1$ with imbalance type MAJ and two scoring functions, APS and RAPS, on dataset CIFAR-10. We set UCR of RC3P the same as or better than that of CCP and Cluster-CP for a fair comparison of prediction set size.

Scoring function	Measure	Methods	MAJ				
			$\rho = 0.5$	$\rho = 0.4$	$\rho = 0.3$	$\rho = 0.2$	$\rho = 0.1$
APS	UCR	CCP	0.070 \pm 0.014	0.050 \pm 0.016	0.080 \pm 0.019	0.070 \pm 0.025	0.040 \pm 0.015
		Cluster-CP	0.020 \pm 0.012	0.040 \pm 0.015	0.020 \pm 0.013	0.010 \pm 0.010	0.070 \pm 0.014
		RC3P	0.070 \pm 0.014	0.050 \pm 0.016	0.080 \pm 0.019	0.070 \pm 0.025	0.040 \pm 0.015
	APSS	CCP	1.84 \pm 0.020	1.825 \pm 0.014	1.939 \pm 0.016	2.054 \pm 0.013	2.629 \pm 0.013
		Cluster-CP	1.948 \pm 0.023	1.999 \pm 0.027	2.167 \pm 0.030	2.457 \pm 0.021	3.220 \pm 0.020
		RC3P	1.84 \pm 0.020	1.825 \pm 0.014	1.939 \pm 0.016	2.054 \pm 0.013	2.629 \pm 0.013
RAPS	UCR	CCP	0.070 \pm 0.014	0.050 \pm 0.016	0.080 \pm 0.019	0.070 \pm 0.025	0.040 \pm 0.015
		Cluster-CP	0.020 \pm 0.013	0.040 \pm 0.015	0.020 \pm 0.012	0.010 \pm 0.010	0.070 \pm 0.014
		RC3P	0.070 \pm 0.014	0.050 \pm 0.016	0.080 \pm 0.019	0.070 \pm 0.025	0.040 \pm 0.015
	APSS	CCP	1.840 \pm 0.020	1.825 \pm 0.014	1.940 \pm 0.016	2.055 \pm 0.013	2.632 \pm 0.012
		Cluster-CP	1.948 \pm 0.023	1.999 \pm 0.028	2.168 \pm 0.030	2.458 \pm 0.021	3.219 \pm 0.030
		RC3P	1.840 \pm 0.020	1.825 \pm 0.014	1.940 \pm 0.016	2.055 \pm 0.013	2.632 \pm 0.012

Table 16: Results comparing CCP, cluster-CP, and RC3P with ResNet-20 model under different imbalance ratio $\rho = 0.5, \rho = 0.4, \rho = 0.2$, and $\rho = 0.1$ with imbalance type EXP and two scoring functions, APS and RAPS, on dataset CIFAR-100. We set UCR of RC3P the same as or better than that of CCP and Cluster-CP for a fair comparison of prediction set size.

Scoring function	Measure	Methods	EXP				
			$\rho = 0.5$	$\rho = 0.4$	$\rho = 0.3$	$\rho = 0.2$	$\rho = 0.1$
APS	UCR	CCP	0.007 \pm 0.002	0.017 \pm 0.004	0.012 \pm 0.004	0.015 \pm 0.003	0.010 \pm 0.002
		Cluster-CP	0.012 \pm 0.002	0.012 \pm 0.003	0.006 \pm 0.002	0.035 \pm 0.008	0.016 \pm 0.004
		RC3P	0.005 \pm 0.002	0.009 \pm 0.001	0.011 \pm 0.003	0.013 \pm 0.003	0.011 \pm 0.002
	APSS	CCP	44.224 \pm 0.341	44.486 \pm 0.420	47.672 \pm 0.463	46.955 \pm 0.402	50.969 \pm 0.345
		Cluster-CP	29.238 \pm 0.609	30.602 \pm 0.553	32.126 \pm 0.563	33.714 \pm 0.863	37.592 \pm 0.857
		RC3P	17.705 \pm 0.004	18.311 \pm 0.005	19.608 \pm 0.007	20.675 \pm 0.005	21.954 \pm 0.005
RAPS	UCR	CCP	0.007 \pm 0.002	0.017 \pm 0.004	0.012 \pm 0.003	0.015 \pm 0.003	0.011 \pm 0.002
		Cluster-CP	0.011 \pm 0.003	0.009 \pm 0.002	0.006 \pm 0.002	0.034 \pm 0.007	0.017 \pm 0.004
		RC3P	0.005 \pm 0.002	0.012 \pm 0.003	0.011 \pm 0.003	0.013 \pm 0.003	0.011 \pm 0.002
	APSS	CCP	44.250 \pm 0.342	44.499 \pm 0.420	47.688 \pm 0.569	46.960 \pm 0.404	50.970 \pm 0.345
		Cluster-CP	29.267 \pm 0.612	30.595 \pm 0.549	32.161 \pm 0.564	33.713 \pm 0.864	37.595 \pm 0.862
		RC3P	17.705 \pm 0.004	18.311 \pm 0.005	19.609 \pm 0.007	20.675 \pm 0.005	21.954 \pm 0.005

Table 17: Results comparing CCP, cluster-CP, and RC3P with ResNet-20 model under different imbalance ratio $\rho = 0.5, \rho = 0.4, \rho = 0.2$, and $\rho = 0.1$ with imbalance type POLY and two scoring functions, APS and RAPS, on dataset CIFAR-100. We set UCR of RC3P the same as or better than that of CCP and Cluster-CP for a fair comparison of prediction set size.

Scoring function	Measure	Methods	POLY				
			$\rho = 0.5$	$\rho = 0.4$	$\rho = 0.3$	$\rho = 0.2$	$\rho = 0.1$
APS	UCR	CCP	0.010 \pm 0.002	0.008 \pm 0.002	0.016 \pm 0.003	0.012 \pm 0.004	0.014\pm 0.003
		Cluster-CP	0.020 \pm 0.003	0.020 \pm 0.002	0.026 \pm 0.004	0.009\pm 0.003	0.034 \pm 0.005
		RC3P	0.009\pm 0.003	0.005\pm 0.002	0.013\pm 0.004	0.011\pm 0.004	0.015 \pm 0.003
	APSS	CCP	49.889 \pm 0.353	54.011 \pm 0.466	56.031 \pm 0.406	59.888 \pm 0.255	64.343 \pm 0.237
		Cluster-CP	38.252 \pm 0.316	39.585 \pm 0.545	43.310 \pm 0.824	47.461 \pm 0.979	52.391 \pm 0.595
		RC3P	23.048\pm 0.008	24.335\pm 0.005	26.366\pm 0.010	28.887\pm 0.006	33.829\pm 0.005
RAPS	UCR	CCP	0.010 \pm 0.002	0.008 \pm 0.002	0.016 \pm 0.003	0.012 \pm 0.004	0.015\pm 0.003
		Cluster-CP	0.019 \pm 0.004	0.020 \pm 0.002	0.026 \pm 0.005	0.009\pm 0.003	0.034 \pm 0.005
		RC3P	0.009\pm 0.003	0.005\pm 0.002	0.013\pm 0.004	0.011 \pm 0.004	0.015\pm 0.003
	APSS	CCP	49.886 \pm 0.353	53.994 \pm 0.467	56.020 \pm 0.406	59.870 \pm 0.253	64.332 \pm 0.236
		Cluster-CP	38.258 \pm 0.320	39.566 \pm 0.549	43.304 \pm 0.549	47.450 \pm 0.969	52.374 \pm 0.592
		RC3P	23.048\pm 0.008	24.335\pm 0.005	26.366\pm 0.010	28.886\pm 0.006	33.185\pm 0.005

Table 18: Results comparing CCP, cluster-CP, and RC3P with ResNet-20 model under different imbalance ratio $\rho = 0.5, \rho = 0.4, \rho = 0.2$, and $\rho = 0.1$ with imbalance type MAJ and two scoring functions, APS and RAPS, on dataset CIFAR-100. We set UCR of RC3P the same as or better than that of CCP and Cluster-CP for a fair comparison of prediction set size.

Scoring function	Measure	Methods	MAJ				
			$\rho = 0.5$	$\rho = 0.4$	$\rho = 0.3$	$\rho = 0.2$	$\rho = 0.1$
APS	UCR	CCP	0.016 \pm 0.003	0.007\pm 0.002	0.017 \pm 0.004	0.010\pm 0.002	0.008\pm 0.004
		Cluster-CP	0.008\pm 0.002	0.012 \pm 0.003	0.021 \pm 0.004	0.021 \pm 0.005	0.019 \pm 0.005
		RC3P	0.016 \pm 0.003	0.010 \pm 0.003	0.015\pm 0.004	0.010\pm 0.002	0.008\pm 0.004
	APSS	CCP	44.194 \pm 0.514	49.231 \pm 0.129	53.676 \pm 0.372	55.024 \pm 0.254	64.642 \pm 0.535
		Cluster-CP	31.518 \pm 0.335	35.355 \pm 0.563	37.514 \pm 0.538	43.619 \pm 0.600	50.883 \pm 0.673
		RC3P	18.581\pm 0.007	21.080\pm 0.010	22.606\pm 0.007	26.785\pm 0.007	32.699\pm 0.005
RAPS	UCR	CCP	0.015 \pm 0.003	0.007\pm 0.002	0.011 \pm 0.004	0.010\pm 0.003	0.008\pm 0.004
		Cluster-CP	0.008\pm 0.003	0.011 \pm 0.003	0.021 \pm 0.004	0.021 \pm 0.002	0.018 \pm 0.005
		RC3P	0.015 \pm 0.003	0.010 \pm 0.003	0.015\pm 0.004	0.010\pm 0.002	0.008\pm 0.004
	APSS	CCP	48.343 \pm 0.353	49.252 \pm 0.128	53.666 \pm 0.371	55.016 \pm 0.254	64.633 \pm 0.535
		Cluster-CP	31.513 \pm 0.325	35.352 \pm 0.547	37.503 \pm 0.535	43.615 \pm 0.608	50.379 \pm 0.684
		RC3P	18.581\pm 0.006	21.080\pm 0.010	22.605\pm 0.007	26.786\pm 0.007	32.699\pm 0.006

Table 19: Results comparing CCP, cluster-CP, and RC3P with ResNet-20 model under different imbalance ratio $\rho = 0.5, \rho = 0.4, \rho = 0.2$, and $\rho = 0.1$ with imbalance type EXP and two scoring function, APS and RAPS, on dataset mini-ImageNet. We set UCR of RC3P the same as or better than that of CCP and Cluster-CP for a fair comparison of prediction set size.

Scoring function	Measure	Methods	EXP				
			$\rho = 0.5$	$\rho = 0.4$	$\rho = 0.3$	$\rho = 0.2$	$\rho = 0.1$
APS	UCR	CCP	0.008 \pm 0.004	0.003 \pm 0.002	0.003 \pm 0.001	0.003 \pm 0.003	0.008 \pm 0.004
		Cluster-CP	0.014 \pm 0.004	0.005 \pm 0.002	0.010 \pm 0.002	0.010 \pm 0.003	0.012 \pm 0.004
		RC3P	0.0\pm 0.0	0.0\pm 0.0	0.0\pm 0.0	0.0\pm 0.0	0.001\pm 0.001
	APSS	CCP	26.676 \pm 0.171	25.663 \pm 0.182	25.941 \pm 0.180	26.127 \pm 0.187	26.111 \pm 0.194
		Cluster-CP	25.889 \pm 0.301	25.878 \pm 0.258	25.680 \pm 0.294	25.522 \pm 0.311	25.253 \pm 0.346
		RC3P	18.129\pm 0.003	17.546\pm 0.002	17.352\pm 0.003	17.006\pm 0.003	17.082\pm 0.002
RAPS	UCR	CCP	0.008 \pm 0.004	0.004 \pm 0.003	0.003 \pm 0.001	0.003 \pm 0.003	0.009 \pm 0.004
		Cluster-CP	0.006 \pm 0.002	0.003 \pm 0.001	0.009 \pm 0.002	0.008 \pm 0.003	0.013 \pm 0.005
		RC3P	0.0\pm 0.0	0.0\pm 0.0	0.0\pm 0.0	0.0\pm 0.0	0.001\pm 0.001
	APSS	CCP	26.756 \pm 0.178	26.621 \pm 0.182	25.021 \pm 0.182	26.216 \pm 0.188	26.212 \pm 0.199
		Cluster-CP	26.027 \pm 0.325	26.000 \pm 0.283	25.922 \pm 0.253	25.564 \pm 0.358	25.415 \pm 0.289
		RC3P	18.129\pm 0.003	17.546\pm 0.002	17.352\pm 0.003	17.006\pm 0.003	17.082\pm 0.002

Table 20: Results comparing CCP, cluster-CP, and RC3P with ResNet-20 model under different imbalance ratio $\rho = 0.5$, $\rho = 0.4$, $\rho = 0.2$, and $\rho = 0.1$ with imbalance type POLY and two scoring function, APS and RAPS, on dataset mini-ImageNet. We set UCR of RC3P the same as or better than that of CCP and Cluster-CP for a fair comparison of prediction set size.

Scoring function	Measure	Methods	POLY				
			$\rho = 0.5$	$\rho = 0.4$	$\rho = 0.3$	$\rho = 0.2$	$\rho = 0.1$
APS	UCR	CCP	0.005 \pm 0.002	0.004 \pm 0.002	0.005 \pm 0.002	0.002 \pm 0.001	0.004 \pm 0.001
		Cluster-CP	0.011 \pm 0.003	0.013 \pm 0.003	0.015 \pm 0.004	0.012 \pm 0.003	0.014 \pm 0.003
		RC3P	0.0\pm 0.0				
	APSS	CCP	26.626 \pm 0.133	26.343 \pm 0.214	27.168 \pm 0.203	27.363 \pm 0.252	26.159 \pm 0.208
		Cluster-CP	26.150 \pm 0.393	25.348 \pm 0.231	26.132 \pm 0.415	26.390 \pm 0.270	25.633 \pm 0.268
		RC3P	17.784\pm 0.003	17.752\pm 0.003	17.652\pm 0.003	17.629\pm 0.003	17.465\pm 0.003
RAPS	UCR	CCP	0.005 \pm 0.002	0.004 \pm 0.002	0.005 \pm 0.002	0.002 \pm 0.001	0.004 \pm 0.002
		Cluster-CP	0.009 \pm 0.003	0.016 \pm 0.004	0.017 \pm 0.004	0.009 \pm 0.003	0.016 \pm 0.003
		RC3P	0.0\pm 0.0				
	APSS	CCP	26.689 \pm 0.142	26.437 \pm 0.213	27.254 \pm 0.201	27.450 \pm 0.249	26.248 \pm 0.219
		Cluster-CP	26.288 \pm 0.407	25.627 \pm 0.318	26.220 \pm 0.432	26.559 \pm 0.242	25.712 \pm 0.315
		RC3P	17.784\pm 0.003	17.752\pm 0.003	17.652\pm 0.003	17.629\pm 0.003	17.465\pm 0.003

Table 21: Results comparing CCP, cluster-CP, and RC3P with ResNet-20 model under different imbalance ratio $\rho = 0.5$, $\rho = 0.4$, $\rho = 0.2$, and $\rho = 0.1$ with imbalance type MAJ and two scoring function, APS and RAPS, on dataset mini-ImageNet. We set UCR of RC3P the same as or better than that of CCP and Cluster-CP for a fair comparison of prediction set size.

Scoring function	Measure	Methods	MAJ				
			$\rho = 0.5$	$\rho = 0.4$	$\rho = 0.3$	$\rho = 0.2$	$\rho = 0.1$
APS	UCR	CCP	0.010 \pm 0.004	0.009 \pm 0.003	0.0\pm 0.0	0.005 \pm 0.002	0.005 \pm 0.002
		Cluster-CP	0.008 \pm 0.002	0.010 \pm 0.000	0.010 \pm 0.003	0.012 \pm 0.004	0.010 \pm 0.003
		RC3P	0.0\pm 0.0				
	APSS	CCP	27.313 \pm 0.154	27.233 \pm 0.246	26.939 \pm 0.177	26.676 \pm 0.267	25.629 \pm 0.207
		Cluster-CP	26.918 \pm 0.241	26.156 \pm 0.255	25.786 \pm 0.356	25.632 \pm 0.383	25.348 \pm 0.334
		RC3P	18.111\pm 0.002	17.874\pm 0.002	18.081\pm 0.003	17.800\pm 0.002	17.167\pm 0.004
RAPS	UCR	CCP	0.009 \pm 0.003	0.009 \pm 0.003	0.0\pm 0.0	0.005 \pm 0.002	0.005 \pm 0.002
		Cluster-CP	0.007 \pm 0.002	0.011 \pm 0.002	0.013 \pm 0.004	0.014 \pm 0.004	0.009 \pm 0.002
		RC3P	0.0\pm (0.0)				
	APSS	CCP	27.397 \pm 0.162	27.320 \pm 0.244	27.013 \pm 0.177	26.782 \pm 0.269	25.725 \pm 0.214
		Cluster-CP	26.969 \pm 0.305	26.293 \pm 0.245	25.956 \pm 0.308	25.803 \pm 0.440	25.532 \pm 0.350
		RC3P	18.111\pm 0.002	17.874\pm 0.002	18.081\pm 0.003	17.800\pm 0.002	17.167\pm 0.004

Table 22: Results comparing CCP, cluster-CP, and RC3P with ResNet-20 model under different imbalance ratio $\rho = 0.5$, $\rho = 0.4$, $\rho = 0.2$, and $\rho = 0.1$ with imbalance type EXP and two scoring function, APS and RAPS, on dataset Food-101. We set UCR of RC3P the same as or better than that of CCP and Cluster-CP for a fair comparison of prediction set size.

Scoring function	Measure	Methods	EXP				
			$\rho = 0.5$	$\rho = 0.4$	$\rho = 0.3$	$\rho = 0.2$	$\rho = 0.1$
APS	UCR	CCP	0.006 \pm 0.002	0.010 \pm 0.002	0.008 \pm 0.002	0.014 \pm 0.004	0.006 \pm 0.002
		Cluster-CP	0.003 \pm 0.002	0.009 \pm 0.003	0.006 \pm 0.003	0.008 \pm 0.003	0.009 \pm 0.003
		RC3P	0.0\pm 0.0				
	APSS	CCP	27.003 \pm 0.183	27.024 \pm 0.162	28.074 \pm 0.199	28.512 \pm 0.154	30.875 \pm 0.163
		Cluster-CP	29.020 \pm 0.281	30.120 \pm 0.440	30.529 \pm 0.381	31.096 \pm 0.350	33.327 \pm 0.440
		RC3P	18.369\pm 0.003	18.339\pm 0.004	18.803\pm 0.003	19.612\pm 0.005	21.556\pm 0.006
RAPS	UCR	CCP	0.006 \pm 0.003	0.010 \pm 0.002	0.008 \pm 0.002	0.014 \pm 0.004	0.006 \pm 0.002
		Cluster-CP	0.004 \pm 0.003	0.010 \pm 0.003	0.006 \pm 0.003	0.010 \pm 0.002	0.012 \pm 0.004
		RC3P	0.0\pm (0.0)				
	APSS	CCP	27.022 \pm 0.192	27.043 \pm 0.163	28.098 \pm 0.199	28.535 \pm 0.155	30.900 \pm 0.170
		Cluster-CP	28.953 \pm 0.333	30.242 \pm 0.466	30.587 \pm 0.377	30.924 \pm 0.317	33.375 \pm 0.377
		RC3P	18.369\pm 0.004	18.339\pm 0.004	18.803\pm 0.003	19.612\pm 0.005	21.556\pm 0.006

Table 23: Results comparing CCP, cluster-CP, and RC3P with ResNet-20 model under different imbalance ratio $\rho = 0.5$, $\rho = 0.4$, $\rho = 0.2$, and $\rho = 0.1$ with imbalance type POLY and two scoring function, APS and RAPS, on dataset Food-101. We set UCR of RC3P the same as or better than that of CCP and Cluster-CP for a fair comparison of prediction set size.

Scoring function	Measure	Methods	POLY				
			$\rho = 0.5$	$\rho = 0.4$	$\rho = 0.3$	$\rho = 0.2$	$\rho = 0.1$
APS	UCR	CCP	0.009 \pm 0.003	0.005 \pm 0.003	0.009 \pm 0.003	0.011 \pm 0.003	0.008 \pm 0.001
		Cluster-CP	0.004 \pm 0.001	0.012 \pm 0.002	0.012 \pm 0.004	0.011 \pm 0.002	0.009 \pm 0.002
		RC3P	0.0\pm 0.0	0.0\pm 0.0	0.0\pm 0.0	0.0\pm 0.0	0.001\pm 0.001
	APSS	CCP	30.943 \pm 0.119	31.239 \pm 0.198	32.283 \pm 0.169	33.570 \pm 0.163	35.912 \pm 0.105
		Cluster-CP	33.079 \pm 0.393	33.951 \pm 0.531	34.626 \pm 0.352	36.546 \pm 0.490	38.301 \pm 0.232
		RC3P	21.499\pm 0.003	21.460\pm 0.005	22.882\pm 0.005	23.708\pm 0.004	25.853\pm 0.004
RAPS	UCR	CCP	0.009 \pm 0.003	0.006 \pm 0.003	0.009 \pm 0.003	0.011 \pm 0.003	0.008 \pm 0.001
		Cluster-CP	0.006 \pm 0.002	0.013 \pm 0.002	0.012 \pm 0.004	0.016 \pm 0.002	0.006 \pm 0.003
	APSS	RC3P	0.0\pm 0.0	0.0\pm 0.0	0.0\pm 0.0	0.0\pm 0.0	0.001\pm 0.001
		CCP	30.966 \pm 0.125	31.257 \pm 0.197	32.302 \pm 0.169	33.595 \pm 0.164	35.940 \pm 0.111
	APSS	Cluster-CP	33.337 \pm 0.409	33.936 \pm 0.448	34.878 \pm 0.282	36.505 \pm 0.520	38.499 \pm 0.216
		RC3P	21.499\pm 0.003	21.460\pm 0.005	22.882\pm 0.005	23.708\pm 0.004	25.853\pm 0.004

Table 24: Results comparing CCP, cluster-CP, and RC3P with ResNet-20 model under different imbalance ratio $\rho = 0.5$, $\rho = 0.4$, $\rho = 0.2$, and $\rho = 0.1$ with imbalance type MAJ and two scoring function, APS and RAPS, on dataset Food-101. We set UCR of RC3P the same as or better than that of CCP and Cluster-CP for a fair comparison of prediction set size.

Scoring function	Measure	Methods	MAJ				
			$\rho = 0.5$	$\rho = 0.4$	$\rho = 0.3$	$\rho = 0.2$	$\rho = 0.1$
APS	UCR	CCP	0.006 \pm 0.001	0.005 \pm 0.002	0.008 \pm 0.003	0.010 \pm 0.002	0.008 \pm 0.002
		Cluster-CP	0.011 \pm 0.003	0.005 \pm 0.002	0.014 \pm 0.004	0.016 \pm 0.004	0.011 \pm 0.002
		RC3P	0.0\pm 0.0				
	APSS	CCP	27.415 \pm 0.194	29.369 \pm 0.120	30.672 \pm 0.182	31.966 \pm 0.165	36.776 \pm 0.132
		Cluster-CP	30.071 \pm 0.412	31.656 \pm 0.261	32.857 \pm 0.469	33.774 \pm 0.494	39.632 \pm 0.342
		RC3P	19.398\pm 0.006	20.046\pm 0.004	21.425\pm 0.003	22.175\pm 0.004	26.585\pm 0.004
RAPS	UCR	CCP	0.006 \pm 0.002	0.005 \pm 0.002	0.008 \pm 0.003	0.010 \pm 0.002	0.008 \pm 0.002
		Cluster-CP	0.011 \pm 0.003	0.005 \pm 0.002	0.013 \pm 0.004	0.014 \pm 0.004	0.014 \pm 0.004
	APSS	RC3P	0.0\pm (0.0)				
		CCP	27.439 \pm 0.203	29.393 \pm 0.120	30.691 \pm 0.182	31.987 \pm 0.165	36.802 \pm 0.138
	APSS	Cluster-CP	29.946 \pm 0.407	31.409 \pm 0.303	32.724 \pm 0.551	33.686 \pm 0.501	39.529 \pm 0.306
		RC3P	19.397\pm 0.006	20.046\pm 0.004	21.425\pm 0.003	22.175\pm 0.004	26.585\pm 0.004

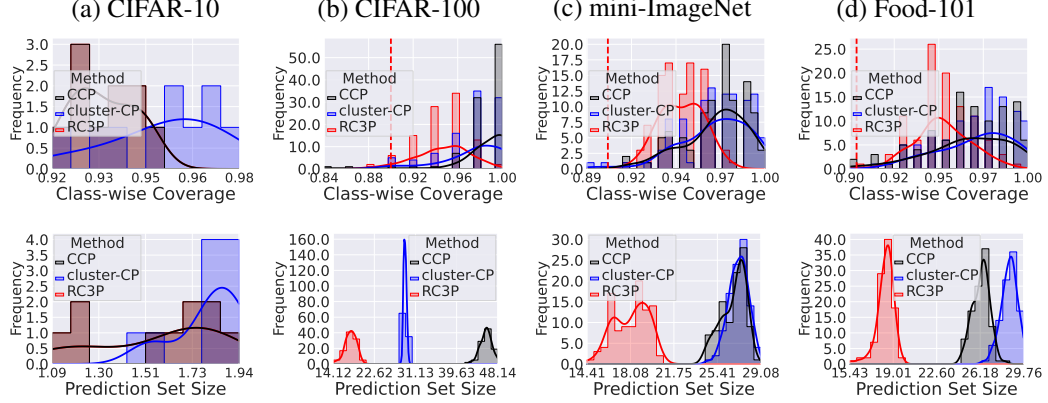


Figure 5: Class-conditional coverage (Top row) and prediction set size (Bottom row) achieved by CCP, Cluster-CP, and RC3P methods when $\alpha = 0.1$ on CIFAR-10, CIFAR-100, mini-ImageNet, and Food-101 datasets with imbalance type EXP for imbalance ratio $\rho = 0.5$. We clarify that RC3P overlaps with CCP on CIFAR-10. It is clear that RC3P has more densely distributed class-conditional coverage above 0.9 (the target $1 - \alpha$ class-conditional coverage) than CCP and Cluster-CP with significantly smaller prediction sets on CIFAR-100, mini-ImageNet and Food-101.

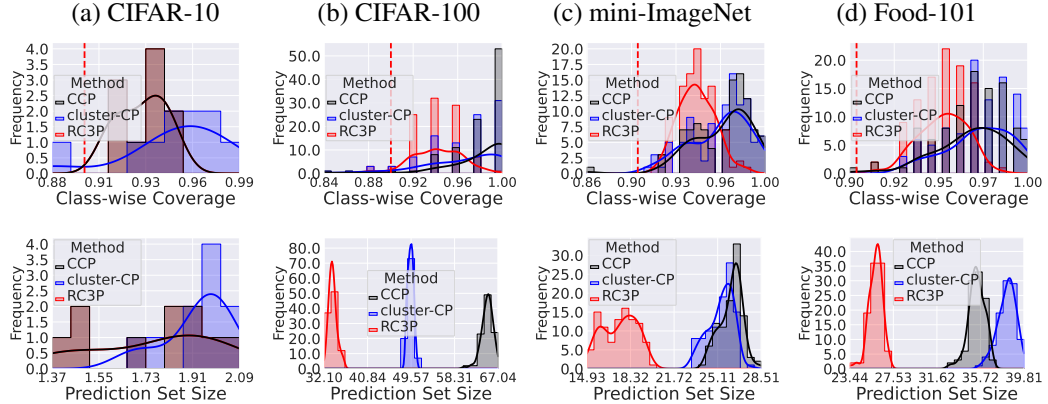


Figure 6: Class-conditional coverage (Top row) and prediction set size (Bottom row) achieved by CCP, Cluster-CP, and RC3P methods when $\alpha = 0.1$ on CIFAR-10, CIFAR-100, mini-ImageNet, and Food-101 datasets with imbalance type POLY for imbalance ratio $\rho = 0.1$. We clarify that RC3P overlaps with CCP on CIFAR-10. It is clear that RC3P has more densely distributed class-conditional coverage above 0.9 (the target $1 - \alpha$ class-conditional coverage) than CCP and Cluster-CP with significantly smaller prediction sets on CIFAR-100, mini-ImageNet and Food-101.

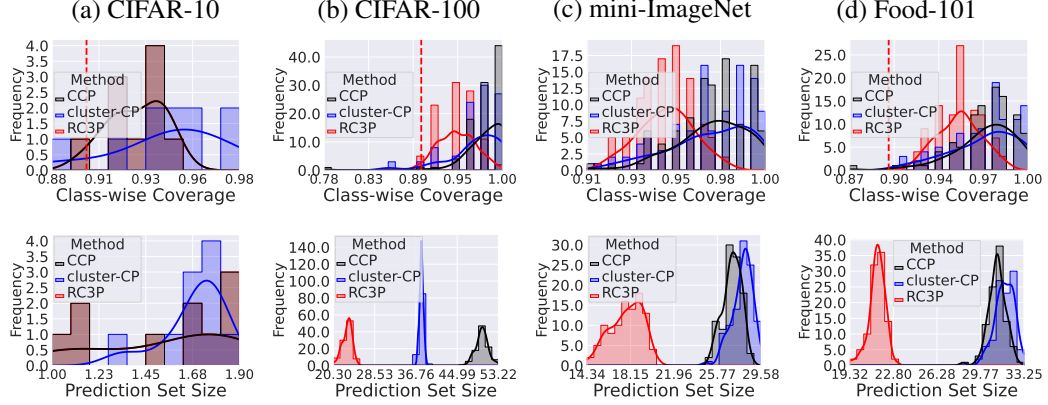


Figure 7: Class-conditional coverage (Top row) and prediction set size (Bottom row) achieved by CCP, Cluster-CP, and RC3P methods when $\alpha = 0.1$ on CIFAR-10, CIFAR-100, mini-ImageNet, and Food-101 datasets with imbalance type POLY for imbalance ratio $\rho = 0.5$. We clarify that RC3P overlaps with CCP on CIFAR-10. It is clear that RC3P has more densely distributed class-conditional coverage above 0.9 (the target $1 - \alpha$ class-conditional coverage) than CCP and Cluster-CP with significantly smaller prediction sets on CIFAR-100, mini-ImageNet and Food-101.

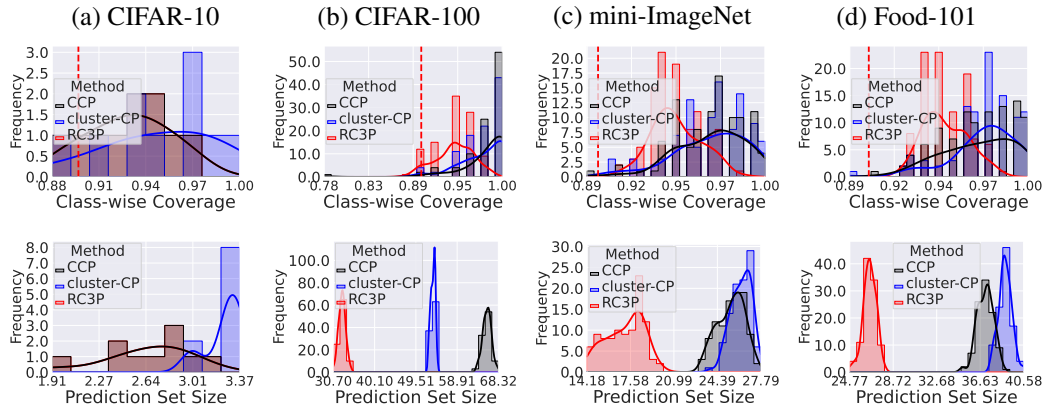


Figure 8: Class-conditional coverage (Top row) and prediction set size (Bottom row) achieved by CCP, Cluster-CP, and RC3P methods when $\alpha = 0.1$ on CIFAR-10, CIFAR-100, mini-ImageNet, and Food-101 datasets with imbalance type MAJ for imbalance ratio $\rho = 0.1$. We clarify that RC3P overlaps with CCP on CIFAR-10. It is clear that RC3P has more densely distributed class-conditional coverage above 0.9 (the target $1 - \alpha$ class-conditional coverage) than CCP and Cluster-CP with significantly smaller prediction sets on CIFAR-100, mini-ImageNet and Food-101.

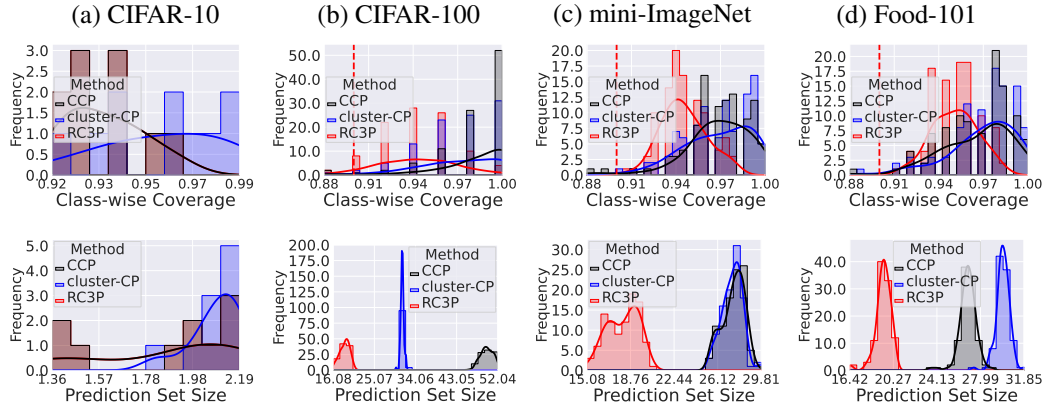


Figure 9: Class-conditional coverage (Top row) and prediction set size (Bottom row) achieved by CCP, Cluster-CP, and RC3P methods when $\alpha = 0.1$ on CIFAR-10, CIFAR-100, mini-ImageNet, and Food-101 datasets with imbalance type MAJ for imbalance ratio $\rho = 0.5$. We clarify that RC3P overlaps with CCP on CIFAR-10. It is clear that RC3P has more densely distributed class-conditional coverage above 0.9 (the target $1 - \alpha$ class-conditional coverage) than CCP and Cluster-CP with significantly smaller prediction sets on CIFAR-100, mini-ImageNet and Food-101.

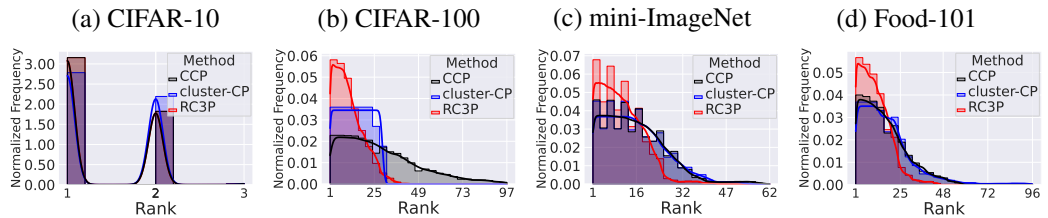


Figure 10: Visualization for the normalized frequency distribution of label ranks included in the prediction set of CCP, Cluster-CP, and RC3P with $\rho = 0.5$ EXP when $\alpha = 0.1$. It is clear that the distribution of normalized frequency generated by RC3P tends to be lower compared to those produced by CCP and Cluster-CP. Furthermore, the probability density function tail for label ranks in the RC3P prediction set is notably shorter than that of other methods.

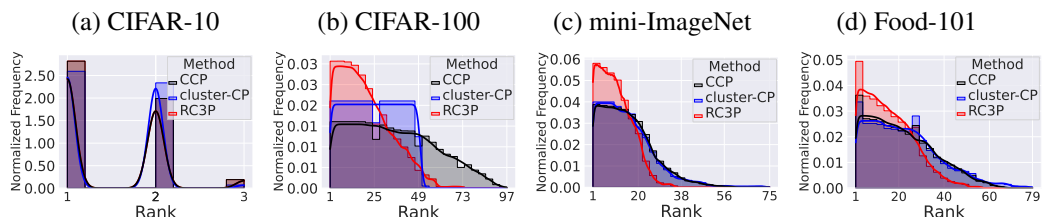


Figure 11: Visualization for the normalized frequency distribution of label ranks included in the prediction set of CCP, Cluster-CP, and RC3P with $\rho = 0.1$ POLY when $\alpha = 0.1$. It is clear that the distribution of normalized frequency generated by RC3P tends to be lower compared to those produced by CCP and Cluster-CP. Furthermore, the probability density function tail for label ranks in the RC3P prediction set is notably shorter than that of other methods.

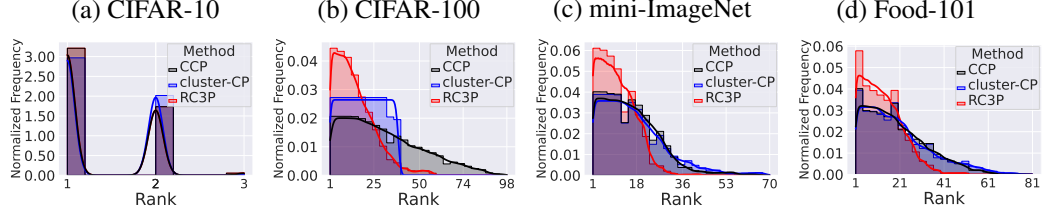


Figure 12: Visualization for the normalized frequency distribution of label ranks included in the prediction set of CCP, Cluster-CP, and RC3P with $\rho = 0.5$ POLY when $\alpha = 0.1$. It is clear that the distribution of normalized frequency generated by RC3P tends to be lower compared to those produced by CCP and Cluster-CP. Furthermore, the probability density function tail for label ranks in the RC3P prediction set is notably shorter than that of other methods.

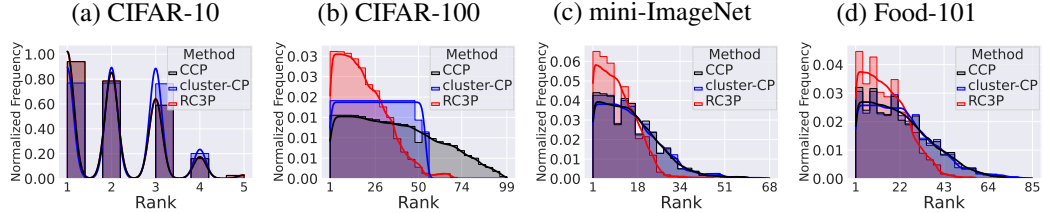


Figure 13: Visualization for the normalized frequency distribution of label ranks included in the prediction set of CCP, Cluster-CP, and RC3P with $\rho = 0.1$ MAJ when $\alpha = 0.1$. It is clear that the distribution of normalized frequency generated by RC3P tends to be lower compared to those produced by CCP and Cluster-CP. Furthermore, the probability density function tail for label ranks in the RC3P prediction set is notably shorter than that of other methods.

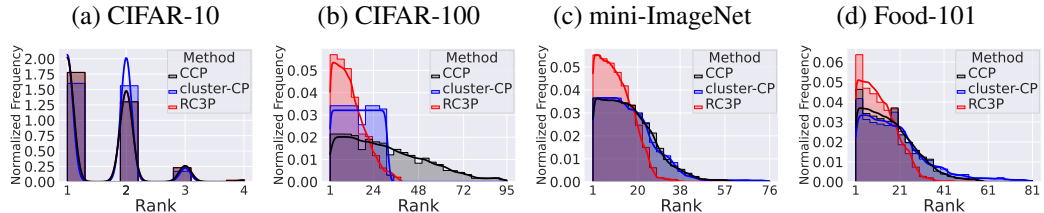


Figure 14: Visualization for the normalized frequency distribution of label ranks included in the prediction set of CCP, Cluster-CP, and RC3P with $\rho = 0.5$ MAJ when $\alpha = 0.1$. It is clear that the distribution of normalized frequency generated by RC3P tends to be lower compared to those produced by CCP and Cluster-CP. Furthermore, the probability density function tail for label ranks in the RC3P prediction set is notably shorter than that of other methods.

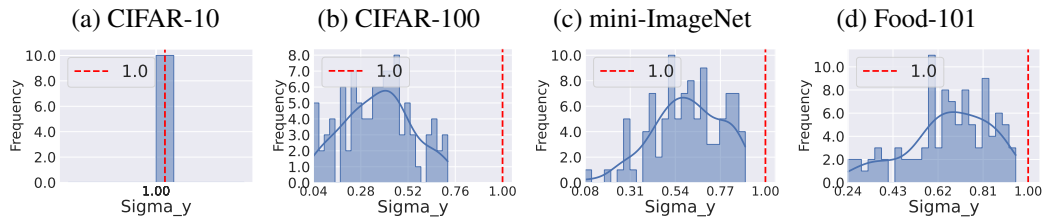


Figure 15: Verification of condition numbers $\{\sigma_y\}_{y=1}^C$ of Equation 6 when epoch = 200 and $\alpha = 0.1$ with $\rho = 0.5$ EXP. Vertical dashed lines represent the value 1, and we observe that all the condition numbers are smaller than 1. This verifies the validity of the condition for Lemma 4.2, and thus confirms that RC3P produces smaller prediction sets than CCP by the optimized trade-off between calibration on non-conformity scores and calibrated label ranks.

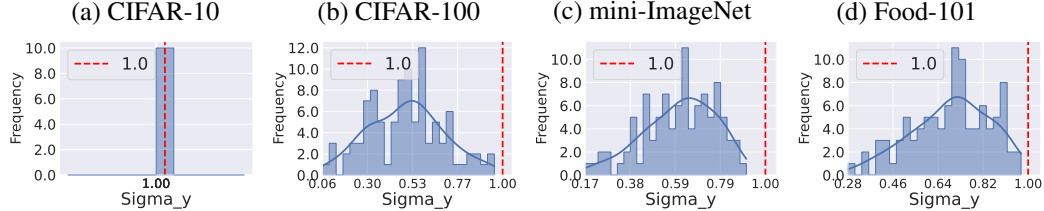


Figure 16: Verification of condition numbers $\{\sigma_y\}_{y=1}^C$ of Equation 6 when epoch = 200 and $\alpha = 0.1$ with $\rho = 0.1$ POLY. Vertical dashed lines represent the value 1, and we observe that all the condition numbers are smaller than 1. This verifies the validity of the condition for Lemma 4.2, and thus confirms that RC3P produces smaller prediction sets than CCP by the optimized trade-off between calibration on non-conformity scores and calibrated label ranks.

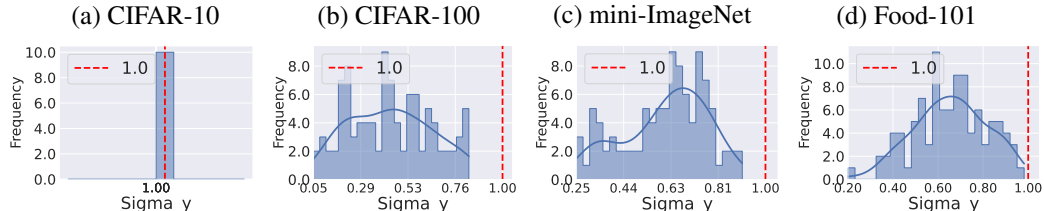


Figure 17: Verification of condition numbers $\{\sigma_y\}_{y=1}^C$ of Equation 6 when epoch = 200 and $\alpha = 0.1$ with $\rho = 0.5$ POLY. Vertical dashed lines represent the value 1, and we observe that all the condition numbers are smaller than 1. This verifies the validity of the condition for Lemma 4.2, and thus confirms that RC3P produces smaller prediction sets than CCP by the optimized trade-off between calibration on non-conformity scores and calibrated label ranks.

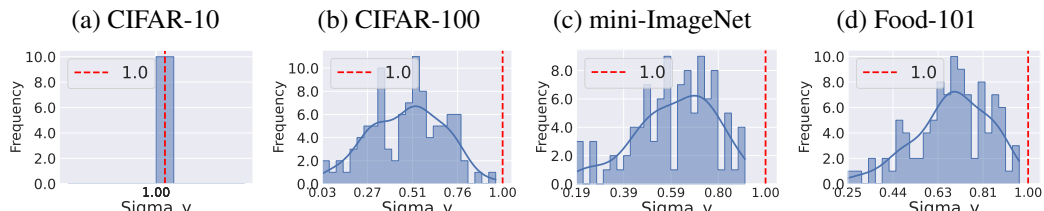


Figure 18: Verification of condition numbers $\{\sigma_y\}_{y=1}^C$ of Equation 6 when epoch = 200 and $\alpha = 0.1$ with $\rho = 0.1$ MAJ. Vertical dashed lines represent the value 1, and we observe that all the condition numbers are smaller than 1. This verifies the validity of the condition for Lemma 4.2, and thus confirms that RC3P produces smaller prediction sets than CCP by the optimized trade-off between calibration on non-conformity scores and calibrated label ranks.

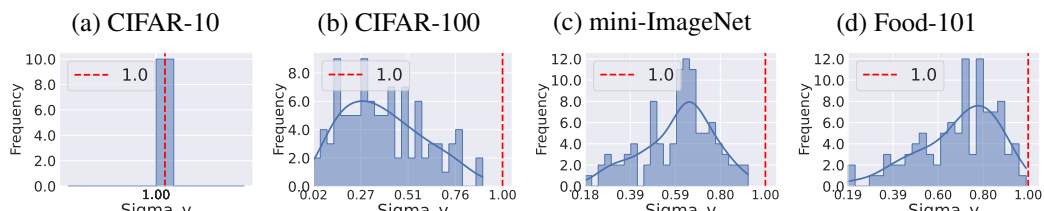


Figure 19: Verification of condition numbers $\{\sigma_y\}_{y=1}^C$ of Equation 6 when epoch = 200 and $\alpha = 0.1$ with $\rho = 0.5$ MAJ. Vertical dashed lines represent the value 1, and we observe that all the condition numbers are smaller than 1. This verifies the validity of the condition for Lemma 4.2, and thus confirms that RC3P produces smaller prediction sets than CCP by the optimized trade-off between calibration on non-conformity scores and calibrated label ranks.

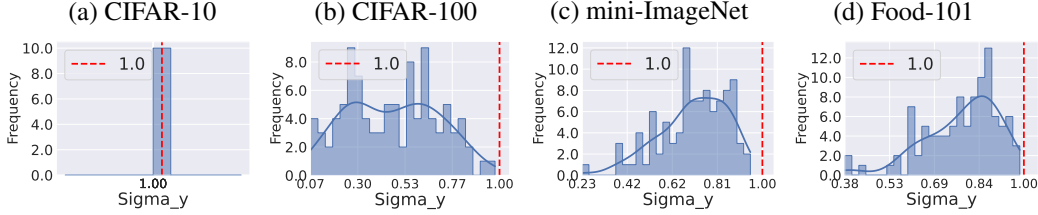


Figure 20: Verification of condition numbers $\{\sigma_y\}_{y=1}^C$ of Equation 6 when epoch = 50 and $\alpha = 0.1$ with $\rho = 0.1$ EXP. Vertical dashed lines represent the value 1, and we observe that all the condition numbers are smaller than 1. This verifies the validity of the condition for Lemma 4.2, and thus confirms that RC3P produces smaller prediction sets than CCP by the optimized trade-off between calibration on non-conformity scores and calibrated label ranks.

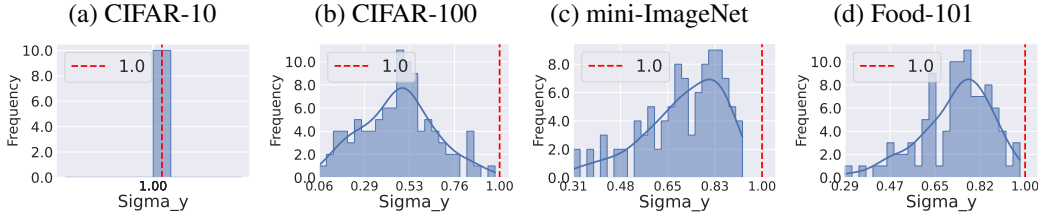


Figure 21: Verification of condition numbers $\{\sigma_y\}_{y=1}^C$ of Equation 6 when epoch = 50 and $\alpha = 0.1$ with $\rho = 0.5$ EXP. Vertical dashed lines represent the value 1, and we observe that all the condition numbers are smaller than 1. This verifies the validity of the condition for Lemma 4.2, and thus confirms that RC3P produces smaller prediction sets than CCP by the optimized trade-off between calibration on non-conformity scores and calibrated label ranks.

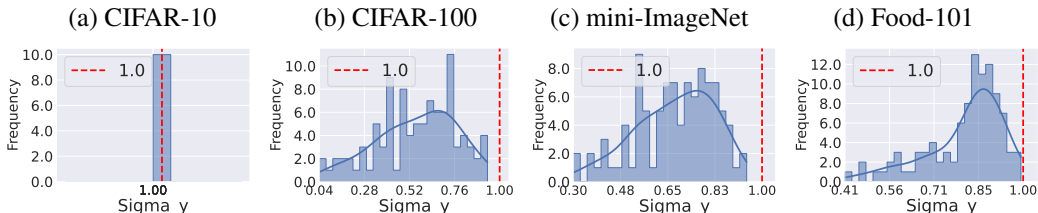


Figure 22: Verification of condition numbers $\{\sigma_y\}_{y=1}^C$ of Equation 6 when epoch = 50 and $\alpha = 0.1$ with $\rho = 0.1$ POLY. Vertical dashed lines represent the value 1, and we observe that all the condition numbers are smaller than 1. This verifies the validity of the condition for Lemma 4.2, and thus confirms that RC3P produces smaller prediction sets than CCP by the optimized trade-off between calibration on non-conformity scores and calibrated label ranks.

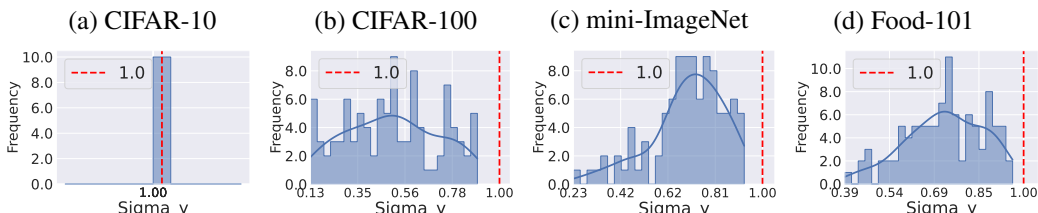


Figure 23: Verification of condition numbers $\{\sigma_y\}_{y=1}^C$ of Equation 6 when epoch = 50 and $\alpha = 0.1$ with $\rho = 0.5$ POLY. Vertical dashed lines represent the value 1, and we observe that all the condition numbers are smaller than 1. This verifies the validity of the condition for Lemma 4.2, and thus confirms that RC3P produces smaller prediction sets than CCP by the optimized trade-off between calibration on non-conformity scores and calibrated label ranks.

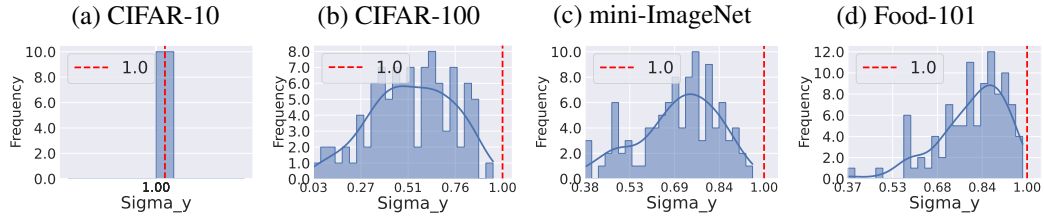


Figure 24: Verification of condition numbers $\{\sigma_y\}_{y=1}^C$ of Equation 6 when epoch = 50 and $\alpha = 0.1$ with $\rho = 0.1$ MAJ. Vertical dashed lines represent the value 1, and we observe that all the condition numbers are smaller than 1. This verifies the validity of the condition for Lemma 4.2, and thus confirms that **RC3P** produces smaller prediction sets than **CCP** by the optimized trade-off between calibration on non-conformity scores and calibrated label ranks.

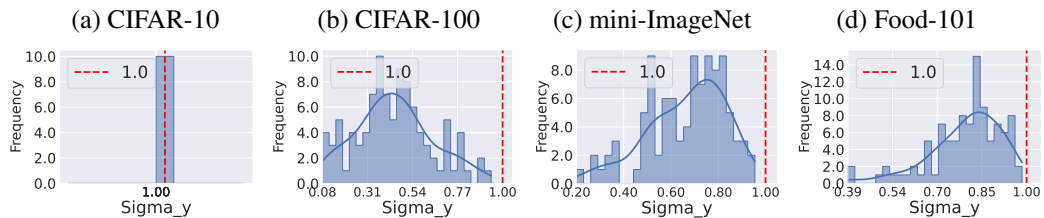


Figure 25: Verification of condition numbers $\{\sigma_y\}_{y=1}^C$ of Equation 6 when epoch = 50 and $\alpha = 0.1$ with $\rho = 0.5$ MAJ. Vertical dashed lines represent the value 1, and we observe that all the condition numbers are smaller than 1. This verifies the validity of the condition for Lemma 4.2, and thus confirms that **RC3P** produces smaller prediction sets than **CCP** by the optimized trade-off between calibration on non-conformity scores and calibrated label ranks.

B.11 Complete Experiment Results on Balanced Classification Datasets

In this subsection, we report complete experimental results over four balanced datasets and $\alpha = 0.1$. Specifically, Figure 26 shows the class-conditional coverage and the corresponding prediction set sizes. From the first row of Fig 26, the class-wise coverage bars of CCP and RC3P distribute on the right-hand side of the target probability $1 - \alpha$ (red dashed line). Second, RC3P outperforms CCP and Cluster-CP with 24.47% (on four datasets) or 32.63% (excluding CIFAR-10) on imbalanced datasets and 32.63% on balanced datasets decrease in terms of average prediction set size the same class-wise coverage. The second row of Figure 26 shows (i) RC3P has more concentrated class-wise coverage distribution than CCP and Cluster-CP; (ii) the distribution of prediction set sizes produced by RC3P is globally smaller than that produced by CCP and Cluster-CP, which is justified by a better trade-off number of $\{\sigma_y\}_{y=1}^K$ as shown in Figure 3.

Figure 27 illustrates the normalized frequency distribution of label ranks included in the prediction sets on balanced datasets. It is evident that the distribution of label ranks in the prediction set generated by RC3P tends to be lower compared to those produced by CCP and Cluster-CP. Furthermore, the probability density function tail for label ranks in the RC3P prediction set is notably shorter than that of other methods. This indicates that RC3P more effectively incorporates lower-ranked labels into prediction sets, as a result of its augmented rank calibration scheme.

Figure 28 verifies the condition numbers σ_y on balanced datasets. This result verifies the validity of Lemma 4.2 and Equation 6 and confirm that the optimized trade-off between the coverage with inflated quantile and the constraint with calibrated rank leads to smaller prediction sets.

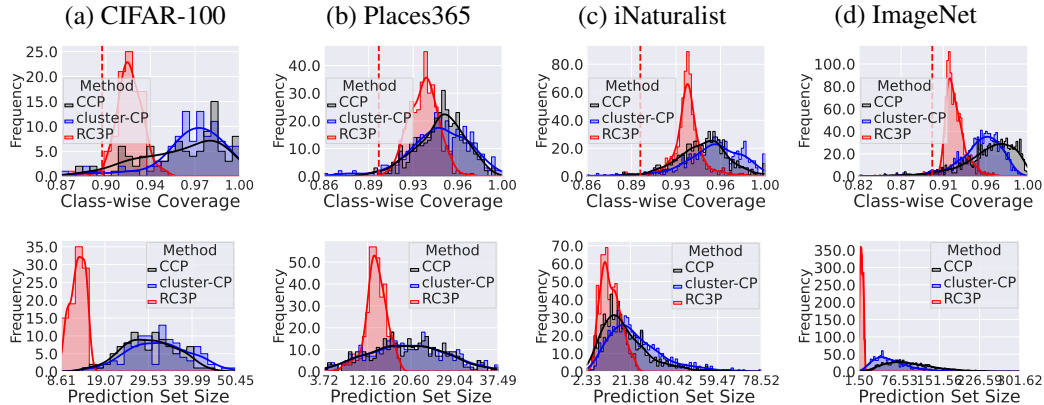


Figure 26: Class-conditional coverage (Top row) and prediction set size (Bottom row) achieved by CCP, Cluster-CP, and RC3P methods when $\alpha = 0.1$ on four balanced datasets. It is clear that RC3P has more densely distributed class-conditional coverage above 0.9 (the target $1 - \alpha$ class-conditional coverage) than CCP and Cluster-CP with significantly smaller prediction sets on all datasets.

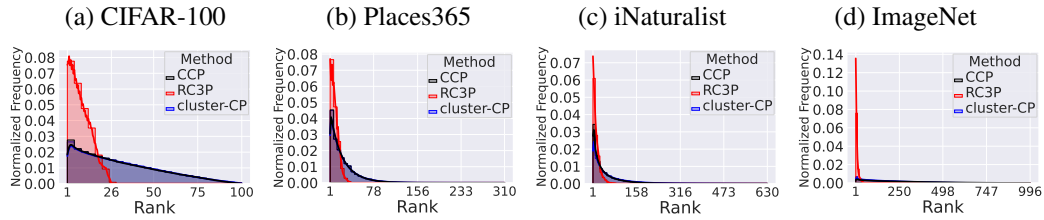


Figure 27: Visualization for the normalized frequency distribution of label ranks included in the prediction set of CCP, Cluster-CP, and RC3P with $\rho = 0.1$ on balanced datasets. It is clear that the distribution of normalized frequency generated by RC3P tends to be lower compared to those produced by CCP and Cluster-CP. Furthermore, the probability density function tail for label ranks in the RC3P prediction set is notably shorter than that of other methods.

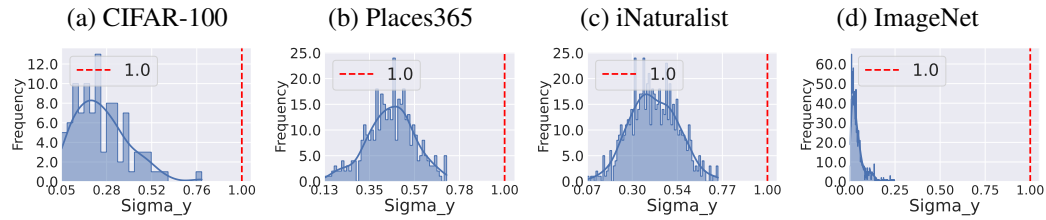


Figure 28: Verification of condition numbers $\{\sigma_y\}_{y=1}^K$ in Equation 6 on balanced datasets. Vertical dashed lines represent the value 1, and we observe that all the condition numbers are smaller than 1. This verifies the validity of the condition for Lemma 4.2, and thus confirms that RC3P produces smaller prediction sets than CCP using calibration on both non-conformity scores and label ranks.